Application of Fractional Order Controllers on Experimental and Simulation Model of Hydraulic Servo System

M. El-Sayed M. Essa, Magdy A.S. Aboelela and M.A.M. Hassan

Abstract Hydraulic Servo System (HSS) plays an important role in industrial applications and other fields such as plastic injection machine, material testing machines, flight simulator and landing gear system of the aircraft. The main reason of using hydraulic systems in many applications is that, it can provide a high torque and high force. The hydraulic control problems can be classified into force, position, acceleration and velocity problems. This chapter presents a study of using fractional order controllers for a simulation model and experimental position control of hydraulic servo system. It also presents an implementation of a non-linear simulation model of Hydraulic Servo System (HSS) using MATLAB/SIMULINK based on the physical laws that govern the studied system. A simulation model and experimental hardware of hydraulic servo system have been implemented to give an acceptable closed loop control system. This control system needs; for example, a conventional controller or fractional order controller to make a hydraulic system stable with acceptable steady state error. The utilized optimization techniques for tuning the proposed fractional controller are Genetic Algorithm (GA). The utilized simulation model in this chapter describes the behavior of BOSCH REXROTH of Hydraulic Servo System (HSS). Furthermore the fractional controllers and conventional controllers will be tuned by Genetic Algorithm. In addition, the hydraulic system has a nonlinear effect due to the friction between cylinders and pistons, fluid compressibility and valve dynamics. Due to these effects, the simulation and experimental results show that using fractional order controllers will give better response, minimum performance indices values, better disturbance rejection, and better sinusoidal trajectory than the conventional PID/PI controllers. It also shows

M.E.-S.M. Essa (✉)
IAET, Imbaba Airport, Giza, Egypt
e-mail: mohamed.essa@iaet.edu.eg

M.A.S. Aboelela · M.A.M. Hassan
Faculty of Engineering, Electric Power and Machines Department,
Cairo University, Giza, Egypt
e-mail: aboelelamagdy@gmail.com

M.A.M. Hassan
e-mail: mmustafa_98@hotmail.com; mmustafa@eng.cu.edu.eg

A.T. Azar et al. (eds.), *Fractional Order Control and Synchronization of Chaotic Systems*, Studies in Computational Intelligence 688,
DOI 10.1007/978-3-319-50249-6_10

that the fractional controller based on Genetic Algorithm has the desired robustness to system uncertainties such as the perturbation of the viscous friction, Coulomb friction, and supply pressure.

Keywords Hydraulic servo system · Genetic Algorithm · PID · Fractional order controllers · MATLAB/SIMULINK · BOSCH REXROTH

1 Introduction

Hydraulic control systems are widely used in many industrial fields due to their small size-to-power ratio and the ability to apply very large force and torque. The Hydraulic Servo System (HSS) applications include: manufacturing systems, material test machines, active suspension systems, mining machinery, fatigue testing, paper machines, injection molding machines, robotics, and aircraft fields.

In hydraulic control system, the main purpose of control is to achieve a desirable response from the system. In light of this requirement; the development of the controller has been established for adjusting measured response to be as close as possible to the desired response. The control signal errors are generally compared with velocity, position, force, pressure, and other system parameters. An HSS is a system consisting of motor, servo, controller, power supply, and other system accessories [19]. In HSS, the system controls the cylinder position to track a certain position trajectory values enforced by the operator. The cylinder movement must precisely follow position, speed, and acceleration profiles. Controller tuning was one of the difficulties that has been faced during implementation of the controllers. Many approaches have been developed for tuning the controller response optimally. This ranges from trial and error, root locus, Zeigler Nicholas (ZN) method and evolutionary techniques [33]. Evolutionary techniques have been evolved from observing complex behaviors of human and other animals, event happening in nature and arrive at a mathematical model representing criteria under study [40]. One of the evolutionary techniques is Swarm Intelligence (SI), which models social behavior of organisms living in swarms.

In the field of hydraulic system control, a wide selection of control design techniques and applications have been figured out. Electro-hydraulic problems are classified into many control problems such as:

(a) Position control problems.
(b) Velocity control problems.
(c) Force control problems.

Due to the importance of hydraulic systems in industrial applications, so many researchers have studied HSS. The dynamics of hydraulic systems are highly nonlinear as stated in [39] and the system may be subjected to non-smooth and discontinuous nonlinearities due to directional change of valve opening, friction…

etc. There have been some studies on analysis and implementation of the nonlinear tracking control law for HSS. This provided exponential stability for force tracking and position tracking to furnish an accurate friction model [39].

In this chapter, the experimental setup of cylinder load has different connection with the recent research. There are different types of automatic controllers that have been applied to HSS to give accurate tracking of position, acceleration, pressure and force. A mathematical modeling and simulation of HSS have been implemented to obtain the observed system response with sinusoidal input. It is then used to design a PID controller based on GA as introduced in [20]. The mathematical modeling of HSS and experimental setup have been developed for force tracking control using the nonlinear fuzzy controller as given in [2]. Whilst the using of Particle Swarm Optimization (PSO) to design an optimal robust PI-controller for HSS that achieves both the robustness and performance measures has been explained in [30]. The using of PSO technique has been extended to identify controller's gains for the Scott Russell mechanism as investigated in [16]. The objective of the HSS controller is to give almost a zero steady state error in motion of the actuator and force output. Thus, these requirements have been satisfied by using PSO based on H_∞ loop shaping control for MIMO HSS, as stated in [31]. The enhancement of stability and robustness of HSS by utilizing the fuzzy strategy approximation for antibodies inhibit adjustment function with immune algorithm based on PSO for PID tuning has been presented in [45]. While the study of external torque of hydraulic actuator and then design a controller using modern control theory have been introduced in [41]. The using of Fuzzy Logic Controller (FLC) for position control of electro hydraulic actuator and ant colony optimization technique that is used to attain the best value for parameters of fuzzy neural network has been stated in [25]. The improvement of position tracking performance based on invariance principle and feed-forward compensation is developed by pole-zero placement theory of the system as described in [44]. A hydraulic position servo system control is implemented by utilizing a Particle Swarm Optimization (PSO) algorithm for control PID loops is presented in [35]. The force control of hydraulic servo system is implemented by designing fuzzy controllers to minimize the force overshoot and preserve the load from failure as illustrated in [8]. The two most common approaches that have been developed to compensate the nonlinear behavior of HSS are adaptive control and variable structure control. The acceleration feedback control by using the variable structure controller in the presence of important friction nonlinearities is introduced and described in [7]. A nonlinear controller based on Lyapunov stability theories that considers the valve's dynamics is used for position control of HSS, as stated in [37].

The dynamic characteristics of HSS are usually very complex and highly nonlinear, so a self organizing and self learning fuzzy algorithm for position control of hydraulic servo drive is represented and discussed in [10]. A sliding mode control, enhanced by the fuzzy PI controller to a typical position control of electro-hydraulic system is confirmed in [27]. Whereas the optimization of PID controller parameters and overcomes of the nonlinearities of HSS based on GA are explained in [3].

A simulation Model of position control of HSS with MATLAB/SIMULINK program is performed and the model is verified experimentally using the Data Acquisition card.

The HSS real time consists of the following hydraulic elements:

- Oil tank with capacity of 100 L.
- Pressure, Temperature and Flow Displays.
- Filter for oil return.
- An axial piston pump swash plate type with variable flow rate pump.
- Servo valve with electrical position feedback (−10 to 10 V), Type 4WRSE, both are made by Rexroth Bosch.
- Pressure relief valve.
- Two hydraulic cylinders with face-to-face connection.
- External length measurement (Position transducer).
- Pressure, Temperature and Flow sensors.

The two cylinders are connected in such away to simulate hydraulic symmetric linear actuator. In addition, the nominal oil pressure is 10 Map. The oil pump is driven by three phase electrical motor 5.5 kW at 1500 rpm. The measuring system consists of one length transducer (measurement range 0–500 mm) which is connected to the piston rod. It is supplied from 24 VDC to generate an electrical signal from −10 to 10 V. The measuring signals are acquired by Data Acquisition card (PCI-NI 6014) from National Instruments with sampling rate 200 ski/s, and then sent to the PC-HP with 1 GB RAM, Windows XP operating system on 2.72 GHz processor.

1.1 Objectives of the Chapter

The objectives of The Study can be summarized as:

- Investigate a simulation model for HSS.
- Prepare the HSS for laboratory testing.
- Develop a Genetic Algorithm (GA) based PID/PI and FOPID/FOPI controllers tuning methodology for optimizing the control of simulated HSS and real time HSS.

1.2 Organization of the Chapter

Section 1 presents an introduction to the chapter. While Sect. 2 displays a description of Hydraulic servo system. Section 3 explains the mechanical and experimental setup. Whilst, system controllers design is given in Sect. 4 but the

tuning method of the proposed controllers is displayed in Sect. 5. Section 6 presents application of GA to hydraulic servo system. While conclusion and future work are given in Sects. 7 and 8 respectively.

2 Hydraulic Servo Systems (HSS)

Electro-hydraulic problems are classified into position control problems, velocity control problems and force control problems. The common types of electro-hydraulic servos are [13]:

- Position servo (linear or angular)
- Velocity or speed servo (linear or angular)
- Force or torque servo.

2.1 Modeling and Simulation of HSS

A mathematical model of a HSS is presented, which includes the most non-linear effects that are involved in the hydraulic system. The problem that has been studied is illustrated in Figs. 1 and 2. The objective of the modeling and simulation of the electro-hydraulic servo system is to design a suitable controller for piston position control. In this section a nonlinear model of a HSS is developed by simulation using SIMULINK/MATLAB program. For more details about the same model but for force tracking control that is illustrated and discussed in [2]. The model describes the behavior of a servo system BOSCH REXROTH [22] servo valve and includes the nonlinearities due to friction forces, valve dynamics, oil compressibility and load influence.

Figure 3 illustrates a focus view of hydraulic cylinder connection and real photo of valve and cylinders connection inside the laboratory. An electro hydraulic servo valve under regulated supply pressure P_s drives the double rod cylinder. Two cylinders can achieve a double rod cylinder configuration, which are mounted into

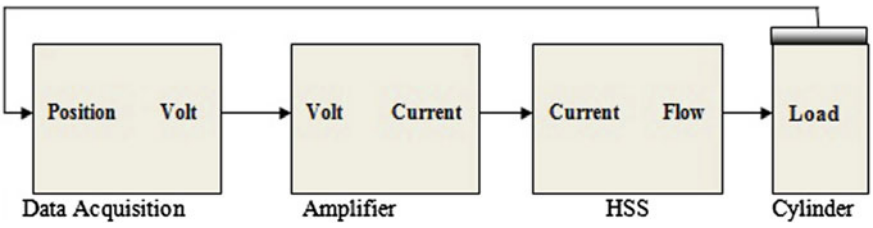

Fig. 1 Block diagram of hydraulic servo system

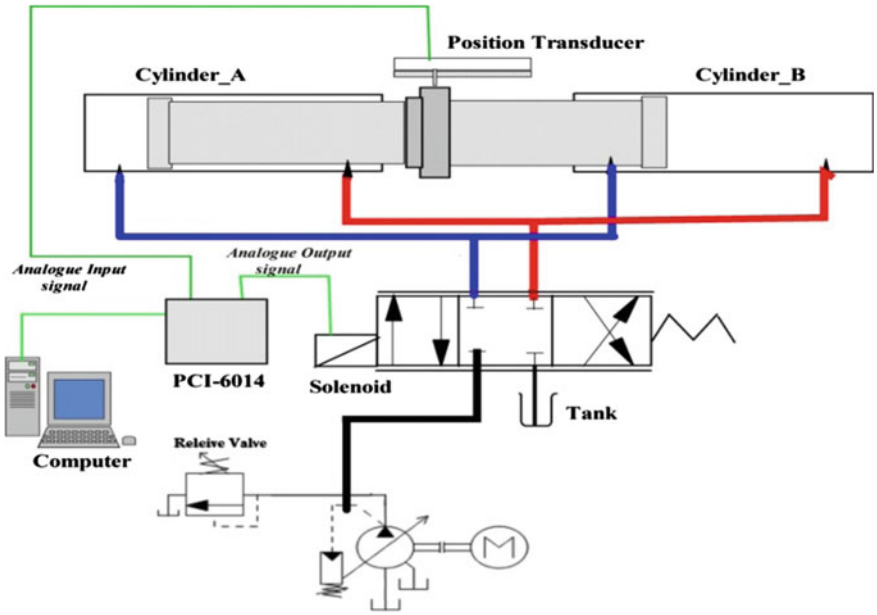

Fig. 2 Schematic diagram of the experimental system

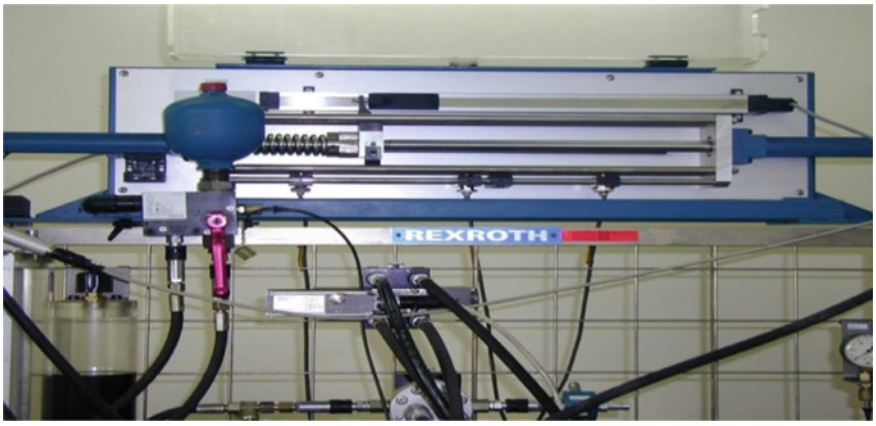

Fig. 3 Real hydraulic servo system

the frame with the face-to-face connection, as illustrated in Fig. 3. The two cylinders are connected in such a way to simulate hydraulic symmetric linear actuator where the piston side of each cylinder is connected to the piston rod side of the other cylinder. The piston position is considered the feedback signal by using linear displacement transducer. The amount of flow rate Q_A in chamber (A) and the

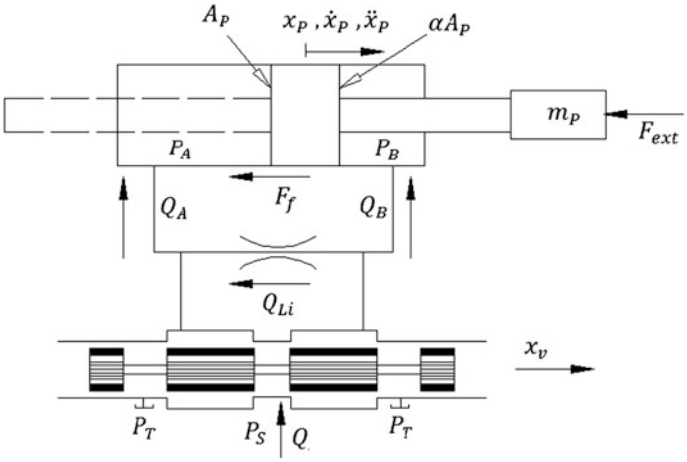

Fig. 4 Valve-cylinder combinations with variables definitions

other amount flow rate Q_B in chamber (B) of the cylinder are function of both the valve spool position x_v and the cylinder pressures P_A and P_B. The objective of this system is to control the piston position of a hydraulic cylinder to track a desired position as closely as possible.

The simplification of nonlinear HSS modeling based on standard assumptions in practical are summarized as:

(1) Low frequency operation.
(2) Pipeline effects do not play a role in the input-output behavior.
(3) Ideal oil supply, constant pressure supply and constant tank pressure.
(4) The possible dynamic behavior of the pressure in the pipelines between valve and actuator is assumed negligible.

Due to the previous assumption, the model of a HSS is composed of two subsystems (valve and cylinder) as shown in Fig. 4 and explained in [12, 15]. The Complete block diagram of HSS is illustrated in Fig. 5.

Where

A_P	Piston area (m^2)
α	Ratio of ring side area to piston side area
m_P	Piston mass (kg)
P_A	Pressure in chamber A (Pa)
P_B	Pressure in chamber B (Pa)
P_S	Supply pressure (Pa)
P_T	Tank pressure (Pa)
Q_A	Flow rate in chamber A (m^3/s)

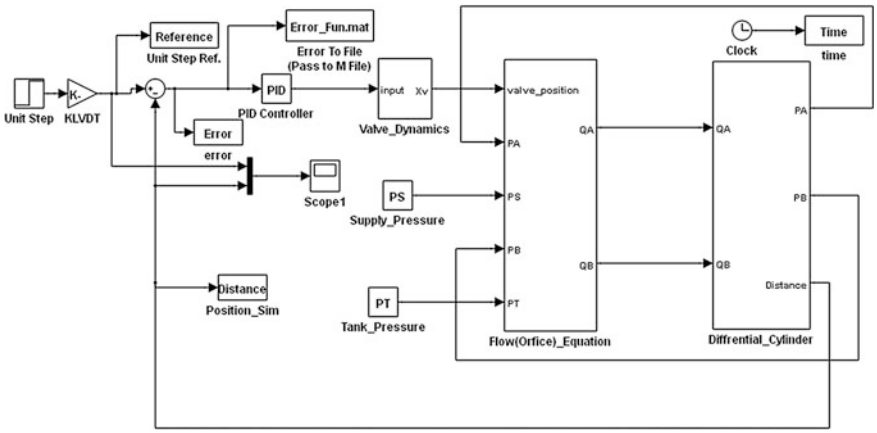

Fig. 5 Complete hydraulic servo system model

Q_B	Flow rate in chamber B (m^3/s)
Q_{Li}, Q_{Le}	Internal and external leakage flow (m^3/s)
$x_P, \dot{x}_P, \ddot{x}_P$	Piston position, velocity, acceleration, respectively (m)
x_v	Valve spool position (m)
F_{ext}	External force (N).

2.1.1 Hydraulic Cylinder Modeling

The hydraulic cylinder includes the pressure, dynamic modeling, the load equally and the piston friction with the cylinder. The differential equations governing the dynamics of the actuator are given in [15, 26]. More details about the hydraulic cylinder modeling can be found in [2, 13]. The total overview of the differential cylinder SIMULINK model is displayed in Fig. 6.

2.1.2 Pressure Dynamics of Hydraulic Chamber

The pressure dynamics equations for the chamber (A) and chamber (B) are displayed in Eqs. (1) and (2).

$$\dot{P}_A = \frac{1}{C_{hA}}(Q_A - A_P\dot{x}_P + Q_{Li} - Q_{LeA}) \tag{1}$$

$$\dot{P}_B = \frac{1}{C_{hB}}(Q_B + \alpha A_P\dot{x}_P - Q_{Li} - Q_{LeB}) \tag{2}$$

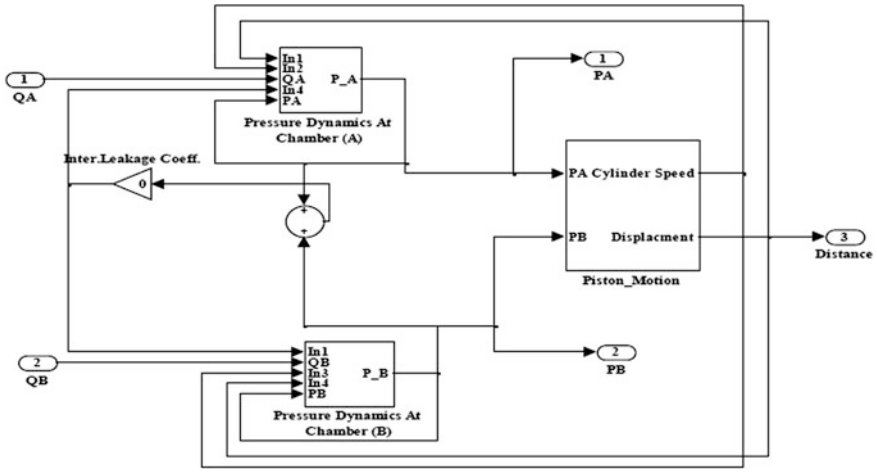

Fig. 6 Block diagram of differential cylinder

where: Q_{Li} is the internal leakage flow. Assume that external leakage flow Q_{LeA} and Q_{LeB} are negligible may be due to the high performance of REXROTH Equipment Company. The hydraulic capacitance of chamber A, C_{hA}, and chamber B, C_{hB}, are given by Eqs. (3) and (4).

$$C_{hA} = C_h(P_A, x_P) = \frac{V_A(x_p)}{\overline{\beta}(P_A)} = \frac{V_{P1,A}(x_{P0} + x_P)A_P}{\overline{\beta}(P_A)} \tag{3}$$

$$C_{hB} = C_h(P_B, x_P) = \frac{V_B(x_p)}{\overline{\beta}(P_B)} = \frac{V_{P1,B}(x_{P0} - x_P)\alpha A_P}{\overline{\beta}(P_B)} \tag{4}$$

$$V_A = V_{P1,A} + \left(\frac{S}{2} + x_P\right)A_P = V_{A0} + x_P A_P \tag{5}$$

$$V_B = V_{P1,B} + \left(\frac{S}{2} - x_P\right)\alpha A_P = V_{B0} - x_P \alpha A_P \tag{6}$$

where: S is the cylinder stroke. $V_{P1,A}$ and $V_{P1,B}$ are the pipeline volumes at A-side and B-side respectively. The initial chamber volumes are assumed that the piston is centered such that these are equal. That is:

$$V_{A0} = V_{B0} = V_0 \tag{7}$$

The commonly used equation for calculation the effective bulk modulus β for hydraulic cylinders is given by Eq. (8) as given in [26].

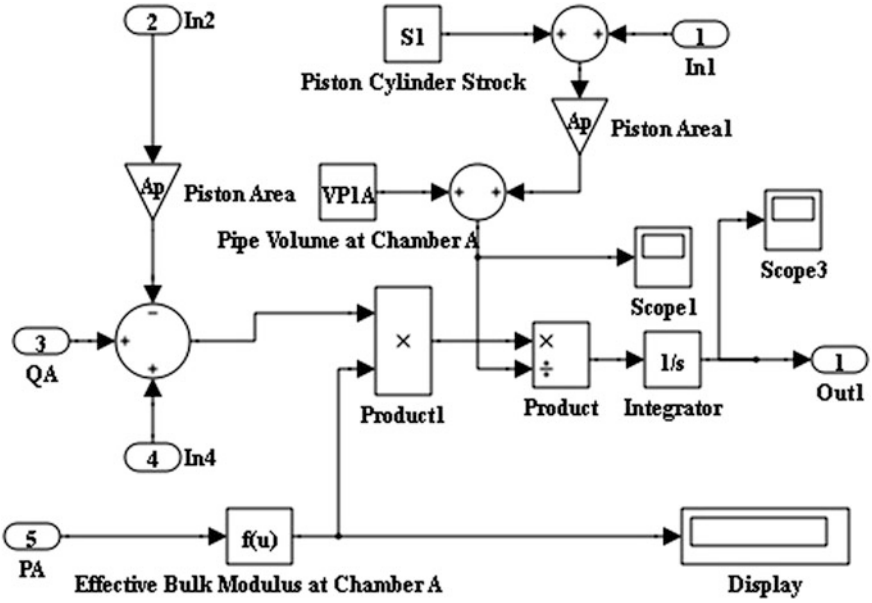

Fig. 7 Pressure dynamics of Side A model

$$\overline{\beta}(p) = a_{1\beta_{max}} \log(a_2 \frac{p}{p_{max}} + a_3) \tag{8}$$

where $a_1 = 50$, $a_2 = 90$, $a_3 = 3$, $\beta_{max} = 1800\,\text{MPa}$, and $p_{max} = 28\,\text{MPa}$. The simulation model of dynamic pressure in chamber A and B are illustrated in Figs. 7 and 8.

2.1.3 Load Equation

Equation (9) illustrates the equation of piston motion which governing the load motion. After applying the Newton's second law to the forces that applied to the piston, the resultant equation is given as follows [15].

$$m_t \ddot{x}_P + K_S x_p + F_f(\dot{x}_P) = (P_A - \alpha P_B) A_P \tag{9}$$

where

K_S Spring stiffness
F_f Friction force
m_t Total mass.

In Eq. (9), there is an external force (F_{ext}) equal to $K_S x_p$ which has been applied as an input force or a disturbing force on the piston. It is achieved by connecting a

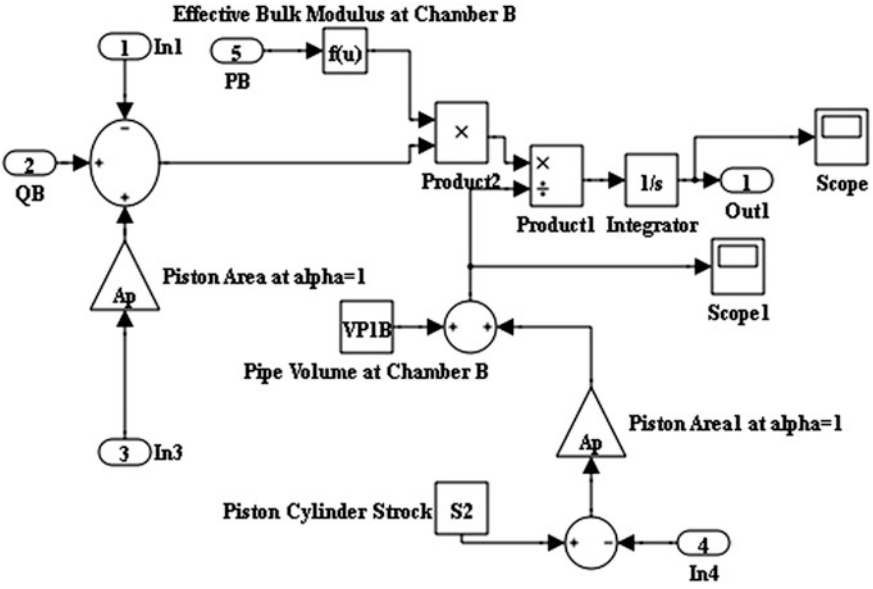

Fig. 8 Pressure dynamics of Side B model

spring at the outer end of the piston. For simplicity, we assume this external force to be zero. This means that, the external force is neglected.

The total mass m_t consists of the piston mass m_P, the mass of hydraulic fluid in the cylinder chambers and in the pipelines, m_{Afl} and m_{Bfl} respectively. Assume the mass of fluid is neglected compared to the piston mass.

$$m_t = m_P + m_{Afl} + m_{Bfl} \tag{10}$$

From Eq. (9) The SIMULINK model of piston, motion is presented in Fig. 9.

2.1.4 Piston Friction

The asymmetry of the friction forces that occurs in differential cylinders can be represented by using one experimental function with referred to stribeck curve as illustrated in Eq. (11). The friction model is shown in Fig. 10 and explained by Jelali and Kroll [15], Merritt [26].

$$F_f(\dot{x}_P) = \left\{ \begin{array}{l} \sigma^+ \dot{x}_P + Sign(\dot{x}_P)\left[F_{CO}^+ + F_{SO}^+ exp\left(-\frac{|\dot{x}_P|}{C_S^+}\right)\right] \forall \dot{x}_P \geq 0 \\ \sigma^- \dot{x}_P + Sign(\dot{x}_P)\left[F_{CO}^- + F_{SO}^- exp\left(-\frac{|\dot{x}_P|}{C_S^-}\right)\right] \forall \dot{x}_P < 0 \end{array} \right\} \tag{11}$$

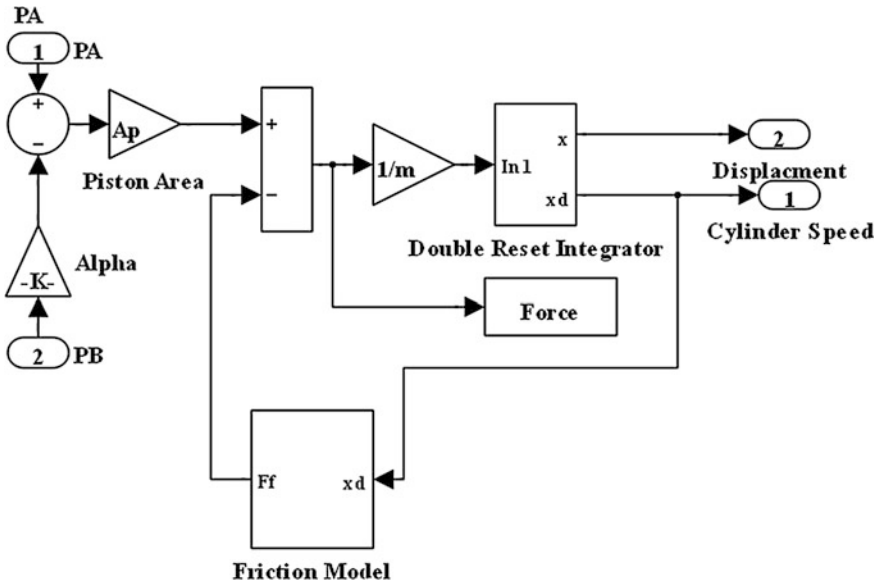

Fig. 9 Piston motion model

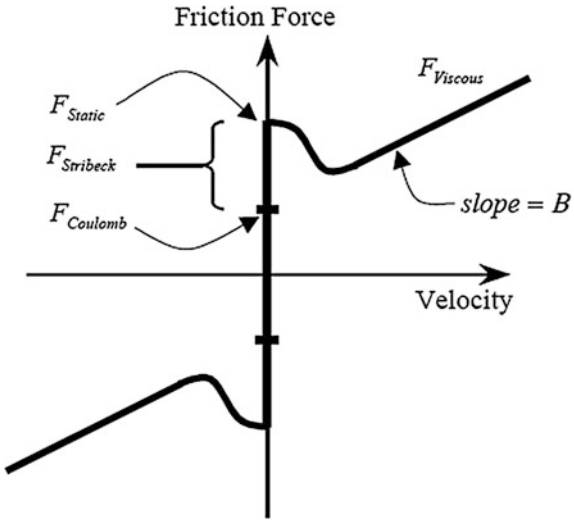

Fig. 10 Friction model

where

σ	Viscous friction parameter
F_{CO}^{+}, F_{CO}^{-}	Differential cylinder Coulomb friction parameter
F_{SO}^{+}, F_{SO}^{-}	Differential cylinder Stribeck friction parameter
C_S^{+}, C_S^{-}	Stribeck velocity range.

An auxiliary force is required to be added to the friction function to prevent the non unique relation between $\dot{x}_P$ and F_f at $\dot{x}_P = 0$ and between x_p and F_c at $x_p = 0$ and then capable to calculate F_f and F_c. More details about auxiliary force are explained in [15]. The friction model SIMULINK block diagram is presented in Fig. 11.

The Figs. 7, 8, 9 and 11 can be arranged to form the total block diagram of a hydraulic cylinder as illustrated in Fig. 6.

2.1.5 Servo Valve Model

The type of the utilized servo valve type (4WRSE) is a four-way spool valve with a critical center, which it is illustrated in Fig. 12.

The classical continuity equation, which governs flow direction in the servo valve, is presented in Eqs. (12), (13), (14) and (15).

$$Q_A = Q_1 - Q_2 \tag{12}$$

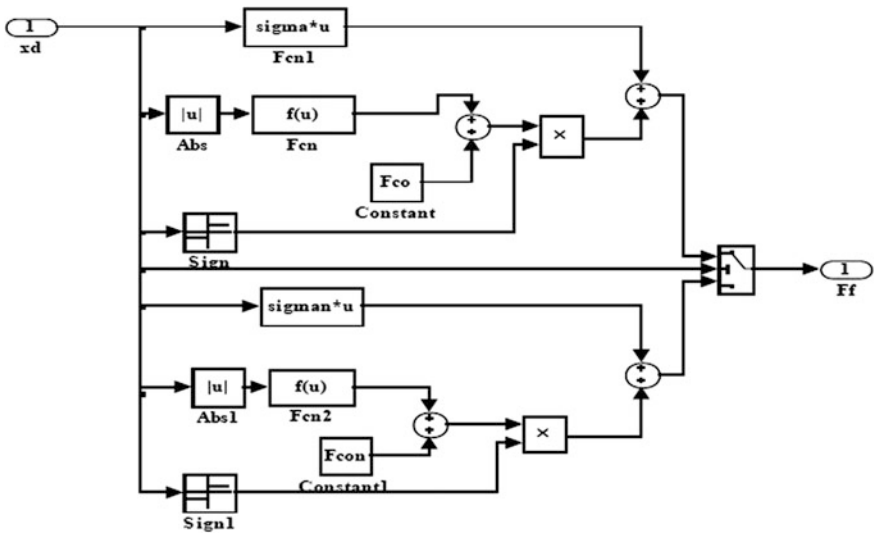

Fig. 11 Friction model diagram

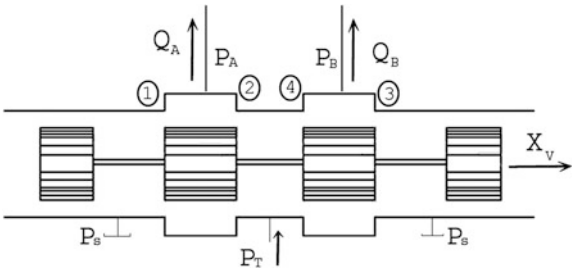

Fig. 12 Zero lapped four ports spool valve

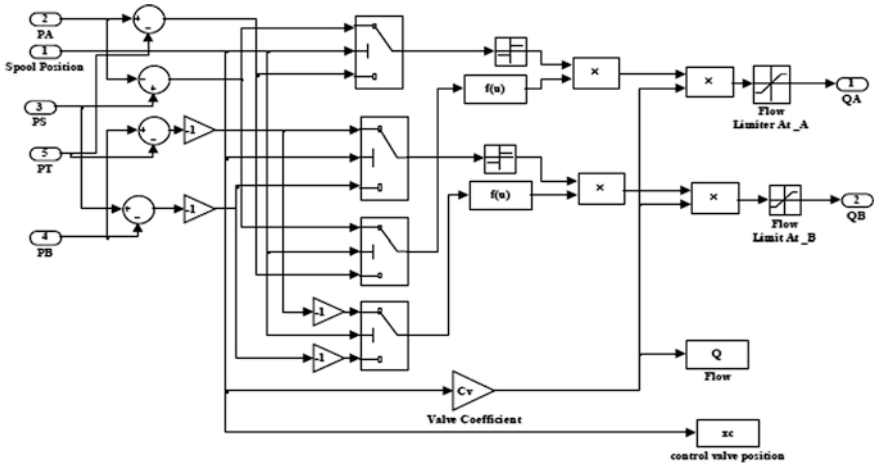

Fig. 13 Simplified block diagram of servo valve

$$Q_A = C_{V1} sg(x_v) Sign(P_S - P_A)\sqrt{|P_S - P_A|} - C_{V2} sg(-x_v) Sign(P_A - P_T)\sqrt{|P_A - P_T|} \tag{13}$$

$$Q_B = Q_3 - Q_4 \tag{14}$$

$$Q_B = C_{V3} sg(-x_v) Sign(P_S - P_B)\sqrt{|P_S - P_B|} - C_{V4} sg(x_v) Sign(P_B - P_T)\sqrt{|P_B - P_T|} \tag{15}$$

where C_{Vi} is a discharge coefficients of the valve orifices and subscript (i) takes a value from 1 to 4 (no. of valve orifice). The C_{Vi} will be equal if all orifices are identical. The definition of function $sg(x)$ is shown in Eq. [16]. Simplified block diagram of servo valve is illustrated in Fig. 13 and is given in [2].

$$sg(x) = \left\{ \begin{array}{ll} x & for \quad x \geq 0 \\ 0 & for \quad x < 0 \end{array} \right\} \tag{16}$$

For simplicity, a first order model for the servo valve is development using system identification toolbox in MATLAB to capture most of dynamic behavior that includes large number of parameters as given in [2, 20]. Equation (17) shows the general form of first order model as given in [2]. The development model of valve dynamics is introduced in Eq. (18).

$$\dot{x}_v = \frac{1}{\tau} x_v + \frac{K_v}{\tau} u \tag{17}$$

where τ is the time constant, K_v is the valve gain and u is the valve input signal. Considering the valve dynamics in Eq. (17) with a time constant 0.0033 s and valve gain 0.98 that yields the resulting transfer function in Eq. (18).

$$\frac{x_v(s)}{u(s)} = K_{Conv.} \frac{300.7}{s + 306.8} \tag{18}$$

where the input u(s) is the command voltage input for the valve and the conversion factor, $K_{Conv.}$ converts the voltage reading out of the valve Linear Variable Differential Transducer (LVDT) to actual spool displacement in meters. The type of valve center is defined by the width of the land compared to the width of the port in the valve sleeve when the spool is in neutral position. The utilized type is a critical-center or zero-lapped valve which has a land width identical to the port width.

At this end, from Eq. (1) to Eq. (17) can be combined to form a total simulated model of HSS. Finally, the complete block diagram of HSS consists of the main following block diagrams.

- Differential Cylinder Block Diagram.
- Valve Dynamics Block Diagram.
- Flow Orifice Block Diagram.

3 Mechanical and Experimental Setup

The hydraulic power unit is illustrated in Fig. 14 and a real time picture of the experimental HSS is illustrated in Fig. 15 and the system components are shown in Fig. 16.

The experimental hydraulic system is mainly consists of the following components as described by [13]:

- Oil tank with capacity of 100 L.
- Pressure, Temperature and Flow Displays.
- Filter for return oil.
- An axial piston pump swash plate type with variable flow rate pump A10VSO.

Fig. 14 Hydraulic power unit

Fig. 15 Real time picture of the experiment HSS

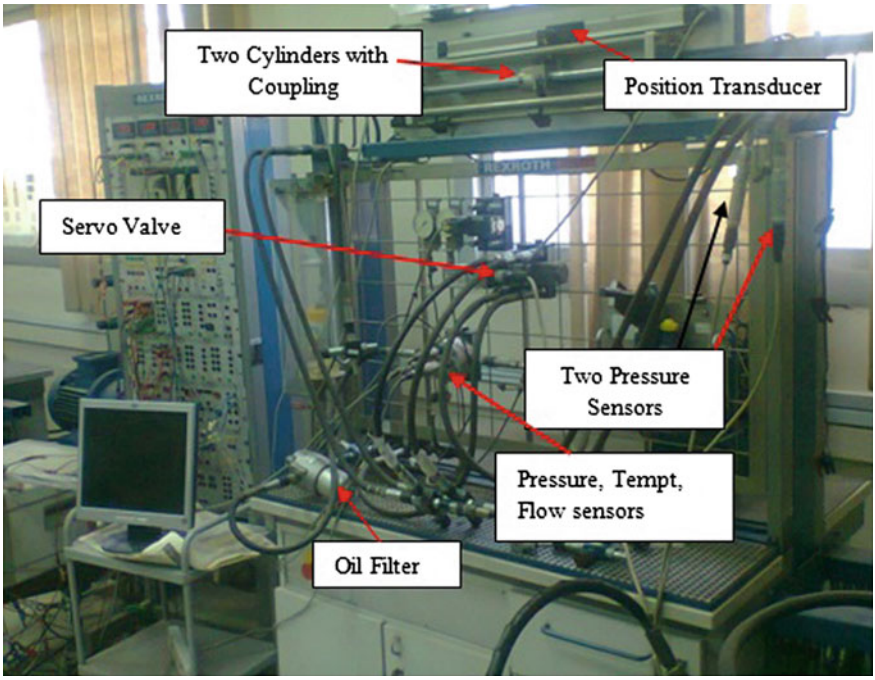

Fig. 16 Real time picture of the experiment components

- Servo valve with electrical position feedback (−10 to 10 V), Type 4WRSE, both are made by Rexroth Bosch.
- Pressure relief valve.
- Two hydraulic cylinders with face-to-face connection.
- External length measurement (Position transducer).
- Pressure, Temperature and Flow sensors.

The main purpose of experimental setup is to verify the simulation model for piston position of HSS and applying the controller design on practical system. Real time photos of the experimental HSS are illustrated in Figs. 14, 15 and 16. In the Experimental system, the two cylinders are connected to simulate hydraulic symmetric linear actuator. The utilized nominal oil pressure is 10 MPa and the oil pump is driven by a three phase electrical motor 5.5 kW at 1500 rpm. The measured system consists of one length transducer has the range of 0–500 mm, which connected to the piston rod, as illustrated in Fig. 15. When a 24 V supplies the transducer, it generates a signal from −10 to 10 V. Data Acquisition Card (PCI-NI 6014) from National Instruments [28] acquires the measuring signals, and then they are sent to the hp-PC with 2.71 GHz processor, 2 GB RAM, and operating system Windows XpSP3. It has a sampling rate (200 kS/s), number of channels (16 single-ended or 8 differential) and 16 bit resolution. The final SIMULINK/MATLAB model of HSS is illustrated in Fig. 17.

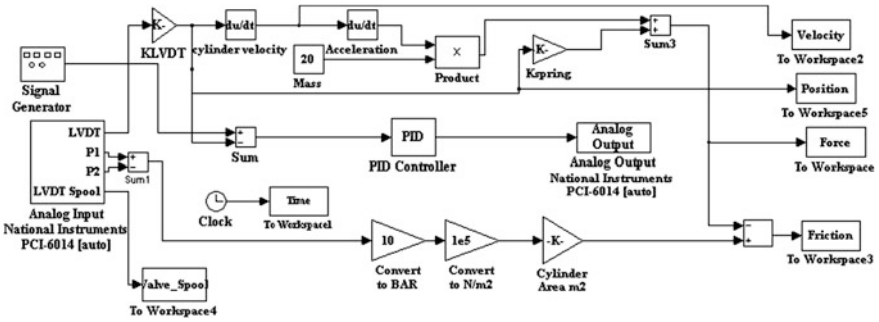

Fig. 17 SIMULINK model of experimental HSS

Fig. 18 System identification

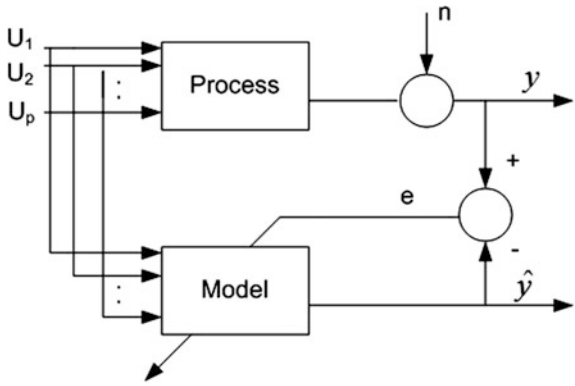

3.1 System Identification

The System Identification allows to build a mathematical models of a dynamic system based on measured data. The model quality is typically measured in terms of the error between the (disturbed) process output and the model output. This error is utilized to adjust the parameters of the model. Schematic diagram of system identification definition is illustrated in Fig. 18 [13, 29].

The main steps that have to be performed for successful identification of a system are illustrated in Fig. 19 and explained in details by Ljung [18].

The purpose of this step is to collect a set of input/output data that describes how the system acts over its entire range of operation. The idea is to motivate the system with a random input u, and observe the impact on the output y.

3.2 Model Representations for System Identification

System identification can be classified into two approaches based on model representation. The first one is input-output model form which is identical to the

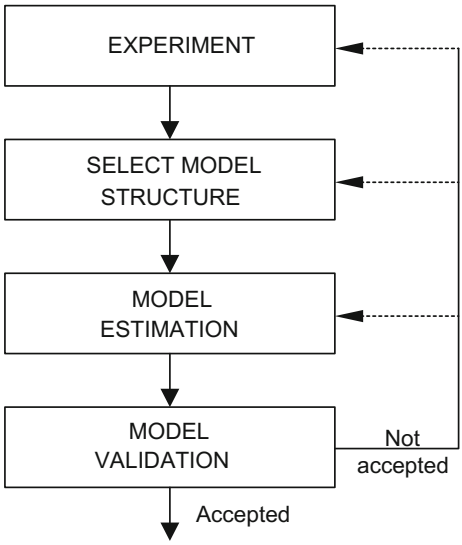

Fig. 19 System identification steps [13]

transfer function representation. The second approach produces models in state space form. Models with state space representation allow identification of multi input multi output (MIMO) systems. The first approach has been utilized in position control of HSS. System Identification Toolbox constructs mathematical models of dynamic systems from measured input-output data. It provides MATLAB functions, SIMULINK blocks, and an interactive tool for creating and using models of dynamic systems not easily modeled from first principles or specifications. Time domain and frequency domain input-output data can be used to identify continuous time, discrete time transfer functions, process models, and state-space models.

3.3 HSS Identification for Position Control

The process models in the system identification toolbox [20] are used to build a continuous time model. It has been used to build and estimate a continuous transfer function for the position control of HSS. Process models consist of the basic type static gain, time constant and time delay as presented in [21]. The mathematical representation of process model is illustrated in Eq. (19). The process model with integrator is described in Eq. (20).

$$P_1(s) = \mathrm{K} \cdot \mathrm{e}^{-\mathrm{T_d} * \mathrm{s}} \frac{1 + \mathrm{T_Z} * \mathrm{s}}{(1 + \mathrm{T_{P1}} * \mathrm{s})(1 + \mathrm{T_{P2}} * \mathrm{s})} \tag{19}$$

$$P_2(s) = \mathrm{K} \cdot \mathrm{e}^{-\mathrm{T_d} * \mathrm{s}} \frac{1 + \mathrm{T_Z} * \mathrm{s}}{\mathrm{s} \cdot (1 + \mathrm{T_{P1}} * \mathrm{s})(1 + \mathrm{T_{P2}} * \mathrm{s})} \tag{20}$$

where the number of real poles (0, 1, 2 or 3) can be determined, as well as the occurrence of a zero in the numerator, the presence of an integrator term (1/s) and the presence of a time delay (Td). In addition, an under damped (complex) pair of poles may replace the real poles. The excitation signal for identification is multi-step signal with variable amplitudes (−2.5 to 2.5 V) and variable frequencies and over arrange of 3000 samples. The first 1500 sample are used to estimate the model while the other 1500 sample are used to the validation step. The experiment is done in closed loop. To calculate the estimated model, the percentage Best Fit (BF) criterion is used as explained in [18]. It measures how much better the model describes the process compared to the mean of the output. The Best Fit description is illustrated in Eq. (21).

$$\text{Best Fit} = \left(1 - \frac{|y - \hat{y}|}{|y - \bar{y}|}\right) \times 100 \tag{21}$$

where y is the measured output, $\hat{y}$ is the simulated or predicted model output, and $\bar{y}$ is the mean of y. A part of measured and simulated outputs is illustrated in Fig. 20 for the identified 3rd order model with integrator. It shows that the model perfectly captures most of the dynamics of the system. The measured and simulated output is illustrated in Fig. 21. The identified continuous-time model here gives Best Fit of 91.88%, which it is an acceptable result.

After the above identification, Eq. (22) introduces the identified continuous time transfer function model and then this equation is discretized to be in z-domain as shown in Eq. (23).

$$\frac{x_P(s)}{u_v(s)} = \frac{1520\,s + 100}{s\,(s^3 + 93.2\,s^2 + 1122\,s + 45.32)} \tag{22}$$

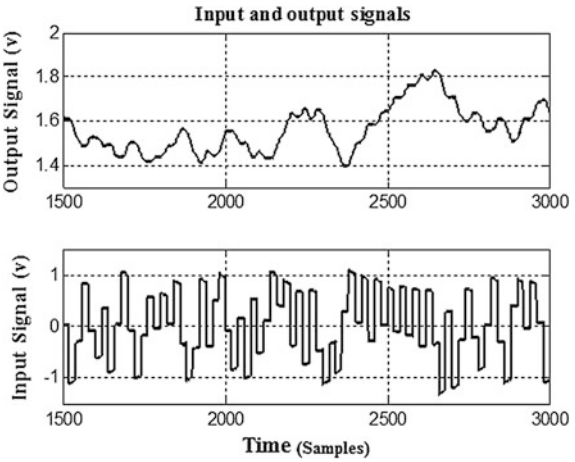

Fig. 20 Input and output signals for HSS identification

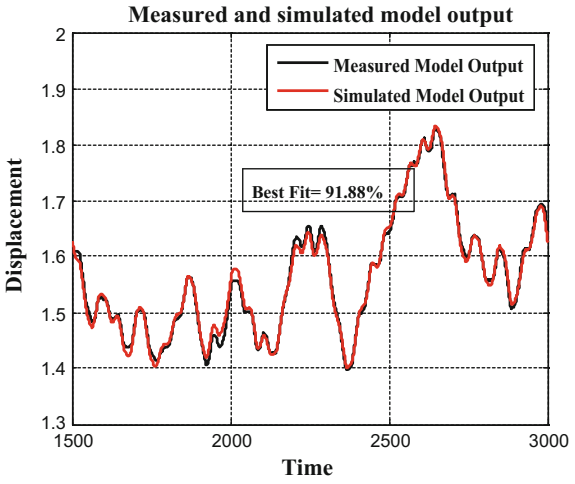

Fig. 21 Measured and simulated model output

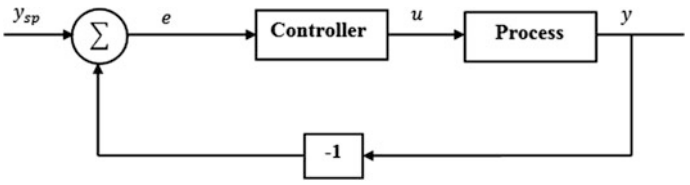

Fig. 22 Block diagram of a process with a feedback controller [12]

$$\frac{x_P(z)}{u_v(z)} = \frac{0.000202\,z^{-1} + 0.0004\,z^{-2} - 0.0005\,z^{-3} - 0.0001\,z^{-4}}{1 - 3.321\,z^{-1} + 4.037\,z^{-2} - 2.109\,z^{-3} + 0.3938\,z^{-4}} \tag{23}$$

4 System Controllers Design

4.1 PID Controller

The PID controller abbreviation is a proportional–Integral–Derivative controller. PID controller is the most common controller form of feedback control system, which is widely used in industrial control systems [43]. The objective of using PID controller is to minimize the difference between a measured process variable and a desired set point by adjusting the process control inputs [5]. Block diagram of a process with a feedback controller is illustrated in Fig. 22 and depicted in [1].

PID controller form is represented mathematically and described by [1, 42]:

$$u(t) = \mathrm{K_p}\left(\mathrm{e(t)} + \frac{1}{\mathrm{T_i}}\int_0^{\mathrm{t}} \mathrm{e}(\tau)\mathrm{d}\tau + \mathrm{T_d}\frac{\mathrm{de(t)}}{\mathrm{dt}}\right) \tag{24}$$

$$u(t) = \mathrm{K_p e(t)} + \mathrm{K_i}\int_0^{\mathrm{t}} \mathrm{e}(\tau)\mathrm{d}\tau + \mathrm{K_d}\frac{\mathrm{de(t)}}{\mathrm{dt}} \tag{25}$$

where

$u(t)$	Controller output
y(t)	System output
$\mathrm{K_p}$, $\mathrm{K_i}$ and $\mathrm{K_d}$	Proportional, Integral and Derivative coefficients respectively
$\mathrm{T_i}$, $\mathrm{T_d}$	Integral and derivative time respectively
e(t)	The system error.

The system error (e(t)) is the difference between the output y(t) and the desired set point as shown in Fig. 22. The mathematical representation of PID controller is displayed in Eqs. (24) and (25).

4.2 Fractional Order PID Controller

Fractional order controller is one of the elegant way that enhance the performance of conventional PID controllers, where integral and derivative actions have, in general, non-integer orders.

In a fractional order controller, besides the proportional, integral and derivative constants, denoted by K_p, K_i and K_d respectively, there are two more adjustable parameters such that the powers of 's' in integral and derivative actions are λ and δ respectively. The values of λ and δ lies between 0 and 1. This provides more flexibility and opportunity to better adjust the dynamical properties of the control system. The fractional order controller revels good robustness. The robustness of fractional controller is more highlighted in presence of a non-linear actuator. The concept of a fractional order PID control system is explained by Das [9], Machado [24], Podlubny [32] and is illustrated in Fig. 23. The fractional order controller is considered as a special case of the classical controller, so that when putting the values of λ and δ equal to 1, it will give the conventional PID controller and when put the values of $\lambda = 1$ and $\delta = 0$, it will give the PI controller.

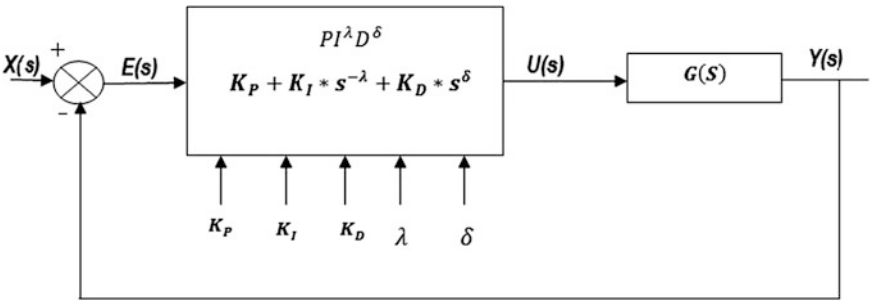

Fig. 23 Fractional order PID control system [13]

Where:

$x(t)$ Input Signal
$e(t)$ Error Signal
$G(s)$ System or Plant Transfer Function
$y(t)$ Output Signal
$u(t)$ Controller Signal.

Fractional order PID controller form is represented mathematically as follows [9]:

$$u(t)_{fc} = K_p \cdot e(t) + K_i \cdot s^{-\lambda} \cdot e(t) + K_d \cdot s^{\delta} \cdot e(t) \tag{26}$$

where: $u(t)_{fc}$ is the controller output and $e(t)$ is the system error.

5 PID and FOPID Controller Tuning

PID controllers and FOPID controller tuning for position control of HSS is designed in this chapter by incorporating Genetic Algorithm (GA). They have been designed and implemented in simulation model of HSS and experimental hardware.

5.1 Genetic Algorithm (GA)

Genetic Algorithm (GA) is an important tool to search and optimize many engineering and scientific problems. These applications includes different fields such that airlines management revenue, artificial creative and automated design for computers and mechatronics. The basic principles of GA were first proposed by Holland [38]. GA is considered as a stochastic optimization algorithm that was originally motivated by the mechanisms of natural selection and evolutionary genetics [6, 38]. It uses a direct analogy of such natural evolution to do global

optimization in order to solve highly complex problems [14]. It supposes that the scope solution of a problem is an individual and can be formed by a set of parameters. These parameters are regarded as the genes of a chromosome and can be structured by concatenated values of string. The form of variables representation is defined by the encoding scheme. But these representations of the variables may be represented by binary, real numbers, or other forms, depending on the application data. Its range is usually defined by the problem.

GA includes a population of individuals, referred to as chromosomes, and each chromosome consists of a string of cells called genes [38]. Chromosomes undergo selection in the presence of variation inducing operators such as crossover and mutation. The crossover in GA occurs with a user specified probability called the "crossover probability" and is problem dependant. The mutation operator is considered to be a background operator that is mainly used to explore new areas within the search space and to add diversity to the population of chromosomes in order to prevent them from being trapped within a local optimum. But the mutation is applied to the offspring chromosomes after crossover is performed. A selection operator selects chromosomes for mating in order to generate offspring. The selection process is usually biased toward fitter chromosomes. A fitness function is used to evaluate chromosomes and reproductive success varies with fitness. The Genetic Algorithm (GA) works on a population using a set of operators that are applied on the population. This population is a set of points in the design space and the initial population is generated randomly by default. Where the next generation of the population is computed using the fitness of the individuals in the current generation.

The genetic algorithm involves a population of individuals called chromosomes where each on represents the solution of the studied problem (parameters of PID/PI and FOPID/FOPI controllers) which its performance is evaluated based on fitness function [11]. A group of chromosomes is selected to undergo to selection, crossover and mutation stages based on the fitness of each individual. The application of selection, crossover and mutation operations yields to create new individuals that give better solutions then the parents leading to optimal solution. The steps of tuning the proposed controllers by GA as follow [36]:

i. Setting of the GA parameters and generate initial, random population of individuals.
ii. Evaluate the fitness function for each chromosome.
iii. Perform selection, crossover and mutation.
iv. Repeat the fitness evaluation until end of generation.

In general, genetic algorithms use some variation of the following procedure to search for an optimal solution [11, 36]:

(a) Initialization
(b) Selection
(c) Crossover
(d) Mutation
(e) Repeat

In the first step (Initialization), an initial population of solutions is randomly generated, and the objective function is estimated for each member of this initial generation as described in [3]. While in the selection step, the individual members are chosen stochastically either to parent the next generation or to be passed on to it. The parent or the passing will occur in the members whose fitness is higher. The solution of fitness based on its objective value which the better objective value means higher fitness. Whereas the cross over means that some of the selected solutions are passed to a crossover operator. The crossover operator combines two or more parents to produce new offspring solutions for the next generation. The crossover operator tends to produce new offspring that keep the common characteristics of the parent solutions, while combining the other behavior in new ways. In this way new areas of the search space are explored, hopefully while retaining

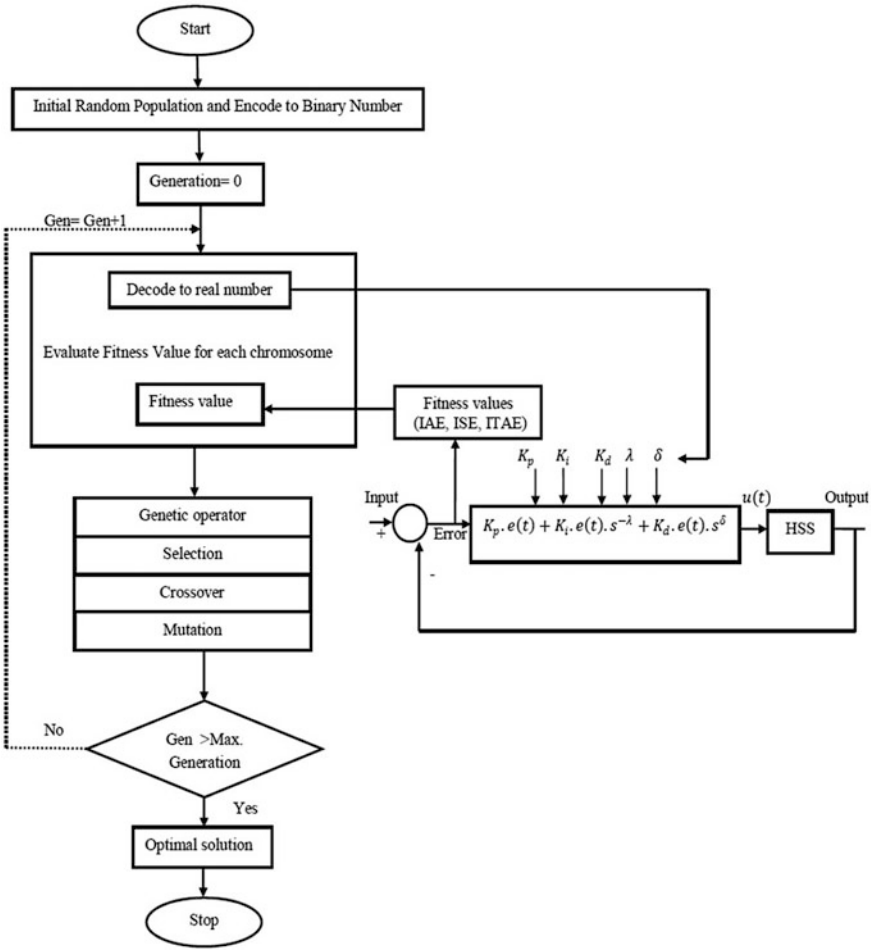

Fig. 24 Flow chart of genetic algorithm for tuning FOPID/FOPI controllers [13]

optimal solution characteristics. In mutation step some of the next-generation solutions are passed to a mutation operator, which introduces random variations in the solutions. The purpose of the mutation operator is to ensure that the solution space is adequately searched to prevent premature convergence to a local optimum. Finally, the current generation of solutions is replaced by the new generation. If the stopping criterion is not satisfied, the process returns to the selection phase. Figure 24 presents the flowchart of GA for tuning PID/PI and FOPID/FOPI controllers as adopted from [36].

6 Application of GA to HSS

6.1 Position Control of HSS

Hydraulic control systems are widely used in many industrial fields, including manufacturing systems; materials test machines, active suspension systems, mining machinery, fatigue testing, flight simulation, paper machines, ships, injection moulding machines, robotics, and aluminum mill equipment. Hydraulic systems are also common in aircraft, where their high power-to-weight ratio [34] and accurate control makes them an ideal choice for actuation of flight surfaces. The control objective is to control the piston position for hydraulic actuator, a PSO, GA, and AWPSO based on PID and FPID controllers have been implemented for piston position control. Error signal acts as an input to the controller. The performance indices (IAE, ISE and ITAE) are used as objective function. The mathematical equations for the performance indices and the cost functions are as follows [4, 23]:

- Integral of Absolute Error (IAE)

$$\mathrm{IAE} = \int_0^\infty |e(t)|dt \tag{27}$$

- Integral of Squared Error (ISE)

$$\mathrm{ISE} = \int_0^\infty e(t)^2 dt \tag{28}$$

- Integral of Time Absolute Error (ITAE)

$$\mathrm{ITAE} = \int_0^\infty t|e(t)|dt \tag{29}$$

For GA the objective function is defined as follows [12, 13, 17]:

$$f = \frac{1}{(performance\ index)} \tag{30}$$

6.2 Parameters of HSS Model

The descriptions and values for position control parameters of HSS model are illustrated in Table 1 [12].

6.3 Simulation Results

The step time of the utilized unit step in the simulation model is 1 s. The settling time, overshoot, undershoot, cross correlation between the reference sinusoidal and output signals of the model, conventional and fractional order gains values for the three performance indices (IAE, ISE and ITAE) are shown in Table 2. The step response and the error of fractional controller and conventional that based on GA with IAE, PID/FOPID and PI/FOPI controllers are shown in Fig. 25. While the

Table 1 Parameters values and description for HSS model

Parameter	Description	Value
A_P	Piston area	0.0012 m^2
C_S^+, C_S^-	Stribeck velocity range	0.015 m/s
C_v	Discharge coefficient of the valve orifices	$9.4281 \times 10^{-5} m^3/s\sqrt{N}$
F_{CO}^+, F_{CO}^-	Cylinder Coulomb friction parameters	300 N, 250 N
K_S	Spring stiffness coefficient	0 N/m
m_t	Total moving mass	20 kg
P_S	Working supply pressure	20 MPa
P_T	Tank pressure	0.1 MPa
P_n	Nominal pressure	10 MPa
Q_n	Nominal flow rate	1.333×10^{-4} m^3/s
S_1, S_2	Cylinder Stroke	0.25 m
$V_{P1,A}, V_{P1,A}$	Pipeline volumes at A-side and B-side	0.000001 m^3
σ^+, σ^-	Cylinder viscous friction parameters	20 N s/m
α	Ratio of ring side area to piston side area	1
F_{SO}^+, F_{SO}^-	Cylinder Stribeck friction parameters	50 N, 120 N
x_{max}, x_{min}	Cylinder stroke limit	±0.28 m
$x_{v,max}$	Maximum valve stroke	$\left\|2 \times 10^{-3}\right\|$ m

Table 2 Simulation results values using GA

Tuning Method	Performance Index	Controller Type	Kp	Integral term		Derivative term		Settling time (sec.)	Over Shoot (%)	XCF(*) Values
				Ki	λ	Kd	δ			
GA	IAE	PID	52.7271	21.97	1	1.21	1	6.39	11.51	0.932
		FOPID	50.3399	23.82	0.05	0.52	0.1	1.65	1.4	0.998
		PI	30.82	13.56	1	0	---	7.20	18.7	0.923
		FOPI	33.0016	12.10	0.14	0	---	2.43	No O.S	0.997
	ISE	PID	53.84	20.74	1	1.47	1	6.64	11.5	0.912
		FOPID	53.5242	20.36	0.01	0.37	0.7	1.64	1.4	0.997
		PI	47.05	17.38	1	0	---	6.92	11.87	0.909
		FOPI	30.6712	12.91	0.27	0	---	2.68	1.4	0.993
	ITAE	PID	51.3985	24.26	1	0.59	1	5.98	14.03	0.895
		FOPID	50.6874	20.51	0.13	0.54	0.3	1.70	0.71	0.998
		PI	42.4784	17.34	1	0	---	6.82	13.66	0.926
		FOPI	30.84	12.66	0.34	0	---	2.79	No O.S	0.996

Where: XCF is the cross correlation coefficient between sinusoidal reference signal and output signal for different techniques.

piston position and the error with ISE based on GA are displayed in Fig. 26. Whilst the step response and the error based on GA with ITAE are illustrated in Fig. 27.

From Table 2, it is visible that the GA for different performance indexes IAE, ISE and ITAE gives different values for the control gains. There are two main reasons for this difference in gains by using different methods and different performance indices. The first one is the different setting of the gains' range for GA in the Matlab code and different setting of the algorithm initial parameters. The user has to consider only positive values of the optimization parameters and consequently a constrained optimization algorithm will be invoked. The way of interaction of this constrained optimization with the initial conditions of each algorithm may also lead to different results. The second reason is the different objective function for the technique, where it may be IAE, or ISE or ITAE.

6.4 Experimental Results

The step time of the utilized unit step in the experimental system is 1 s. The settling time, overshoot, undershoot, cross correlation between the reference sinusoidal and output signals of the model, conventional and fractional order gains values for the three performance indices (IAE, ISE and ITAE) for GA is shown in Table 3. In addition, for the comparison between fractional controller and conventional

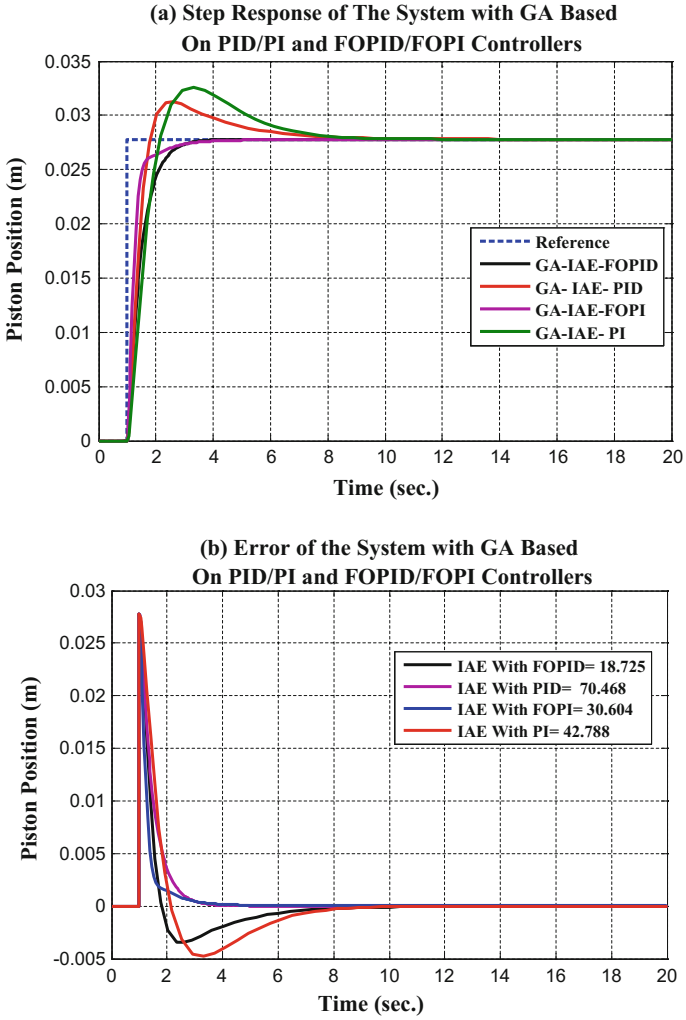

Fig. 25 Piston position and error of HSS simulation model with FOPID/FOPI and PID/PI based on GA and IAE

controller, the step response and the error of system based on GA with IAE, PID/FOPID and PI/FOPI controllers are illustrated in Fig. 28. Whilst the piston position and the error with ISE based on GA are shown in Fig. 29. While the step response and the error based on GA with ITAE are displayed in Fig. 30. The same reasons for parameters different that has been discussed in Sect. 6.3 are the same in the experimental work.

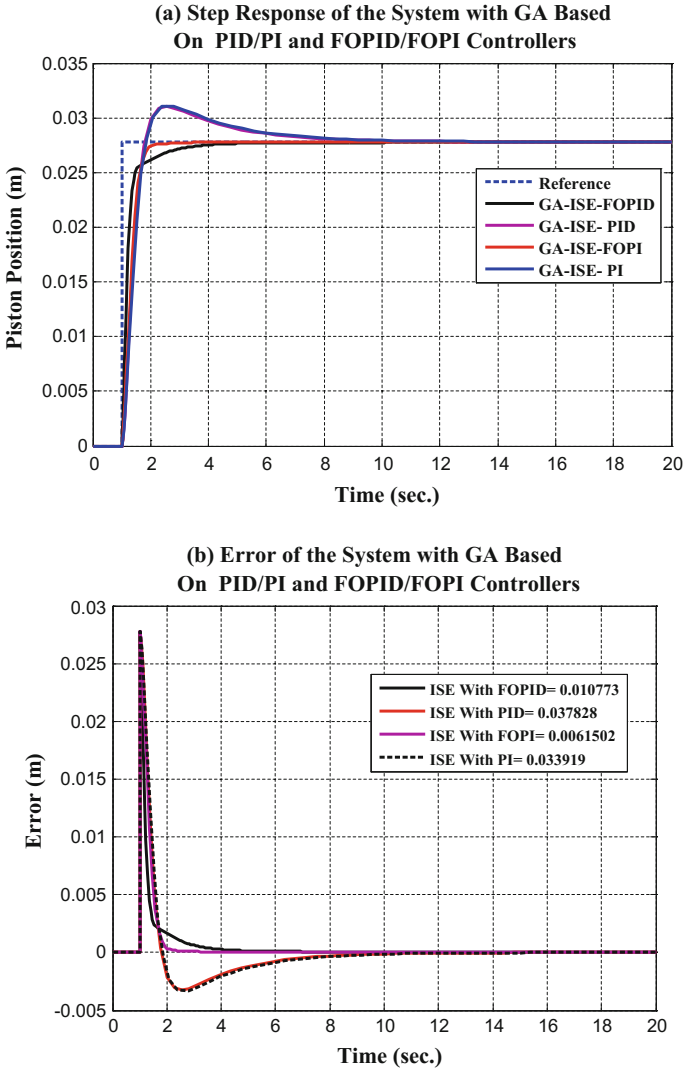

Fig. 26 Piston position and error of HSS simulation model with FOPID/FOPI and PID/PI based on GA and ISE

6.5 Discussion of Simulation Results

The argument of the simulation model depends on the results for GA that have been illustrated in Table 2. In case of IAE, the GA for conventional and fractional controllers gave an acceptable settling time in seconds which are within the permissible range (0–30 s). But due to the nonlinearities of the HSS, the settling time

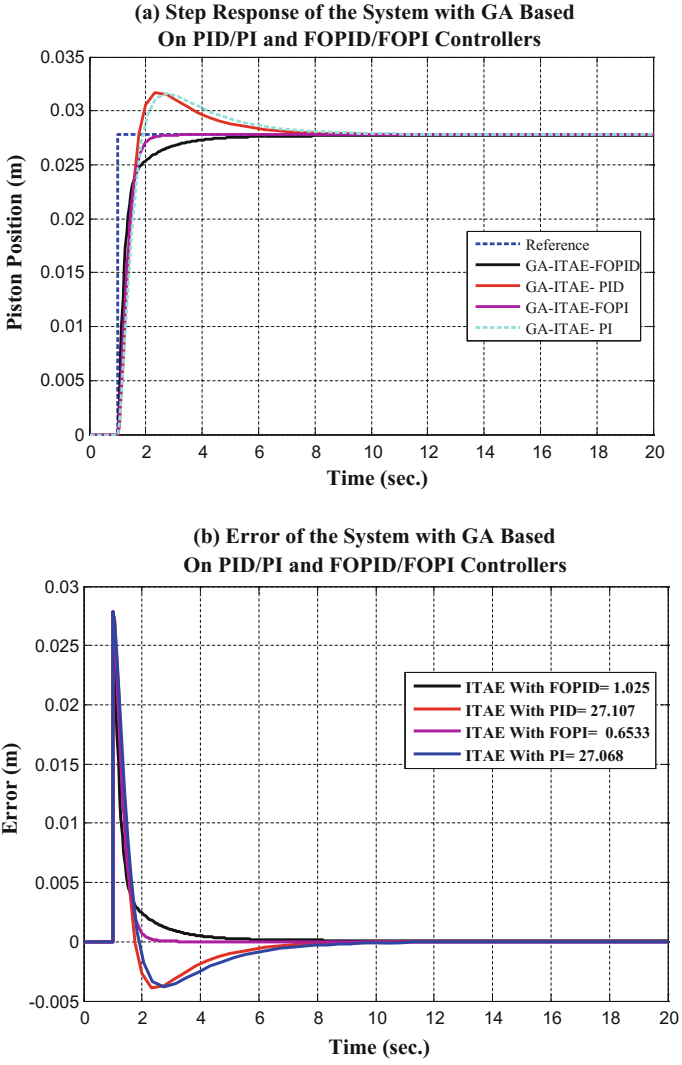

Fig. 27 Piston position and error of HSS simulation model with FOPID/FOPI and PID/PI based on GA and ITAE

of the system response based on fractional order controller is the minimum value which is around 1.5 s compared with the other results. Furthermore the percentage of system overshoot in case of fractional controller is 1% which is the minimum value compared with the other results. While in case of ISE, the GA for conventional and fractional controllers also gave an adequate settling time in seconds which are inside the permissible range (0–30 s). But the settling time of the system response anchored in fractional order controller is the minimum value which is

Table 3 Experimental results values using PSO, AWPSO and GA

Tuning Method	Performance Index	Control-ler Type	Kp	Integral term		Derivative term		Settling time (sec.)	Over Shoot (%)	XCF(*) Values
				Ki	λ	Kd	δ			
GA	IAE	PID	52.7271	21.97	1	1.21	1	6.7327	11.51	0.89
		FOPID	50.3399	23.82	0.05	0.52	0.1	2.22	No O.S	0.92
		PI	30.82	13.56	1	0	---	7.5516	18.7	0.93
		FOPI	33.0016	12.10	0.14	0	---	3.17	1	0.985
	ISE	PID	53.84	20.74	1	1.47	1	7.0548	11.87	0.94
		FOPID	53.5242	20.36	0.01	0.37	0.7	2.07	No O.S	0.98
		PI	47.05	17.38	1	0	---	8.0585	11.87	0.89
		FOPI	30.6712	12.91	0.27	0	---	3.79	0.71	0.91
	ITAE	PID	51.3985	24.26	1	0.59	1	6.4047	14.39	0.89
		FOPID	50.6874	20.51	0.13	0.54	0.3	2.54	No O.S	0.98
		PI	42.4784	17.34	1	0	---	7.336	16.18	0.92
		FOPI	30.84	12.66	0.34	0	---	3.93	0.71	0.95

around 1.5 s in relation to the other types of controllers. In addition, there isn't a system overshoot in case of fractional order controller compared with available system overshoot in conventional controllers. In addition to the results, in case of ITAE, it shows that the used optimization technique 'GA' gave an acceptable settling time values for fractional controllers, which within the permissible range. But the settling time of the system response based on fractional order controller is the minimum value which around 1.5 s compared with the other technique results. Additionally, there isn't a system overshoot in case of fractional order controller compared with available system overshoot in the other Evolutionary techniques.

The simulation results show that, there isn't systems undershoot for the three performance indices (IAE, ISE and ITAE) in the case of using PID/PI and FOPID/FOPI controllers. When using the same mentioned parameters of the PID/PI and FOPID/FOPI controllers in Table 2, the Fractional Order controller that based on GA technique give an efficient sinusoidal wave tracking, where it gives an acceptable cross correlation coefficients. On a global view to the responses, it is found that the nonlinear controller or the fractional order controller based on GA is the better controller than classical controller in determination the optimal parameters of the proposed controller. Moreover, the settling time and system overshoot of the three performance indices in case of Fractional Order PID (FOPID) controller is the minimum value compared with the other results. In fact the fractional controller shows its good performance in reducing the settling time and overshoot from available overshoot value to non overshoot. It is also found that there isn't system undershoot for all the optimization techniques. Furthermore the used FOPID gives a better system response and results compared with FOPI controller results.

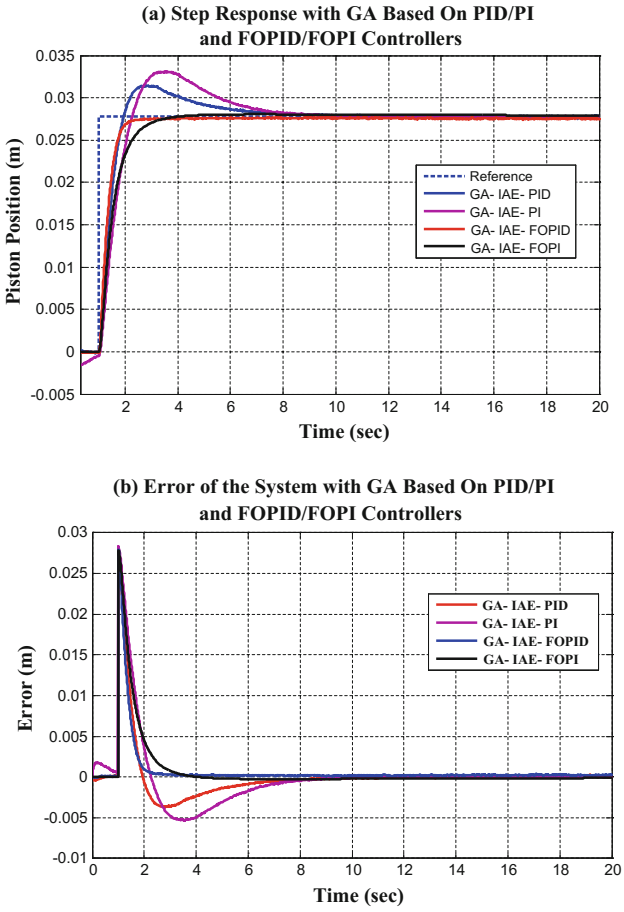

Fig. 28 Piston position and error of experimental HSS with FOPID/FOPI and PID/PI based on GA and IAE

The resultant performance indices that are displayed in the figures must be multiplied by 10^{-3} to get the actual values for the performance indices.

6.6 *Effects of Changing Reference Profile for the Simulation HSS*

A changing of reference profile with 50% of the set point value is added to the control signal (unit step input) at the process input and drive the system away from its desired operating point from (t = 20) seconds to (t = 40) seconds during the stability condition of the system. The changing in profile based on GA with

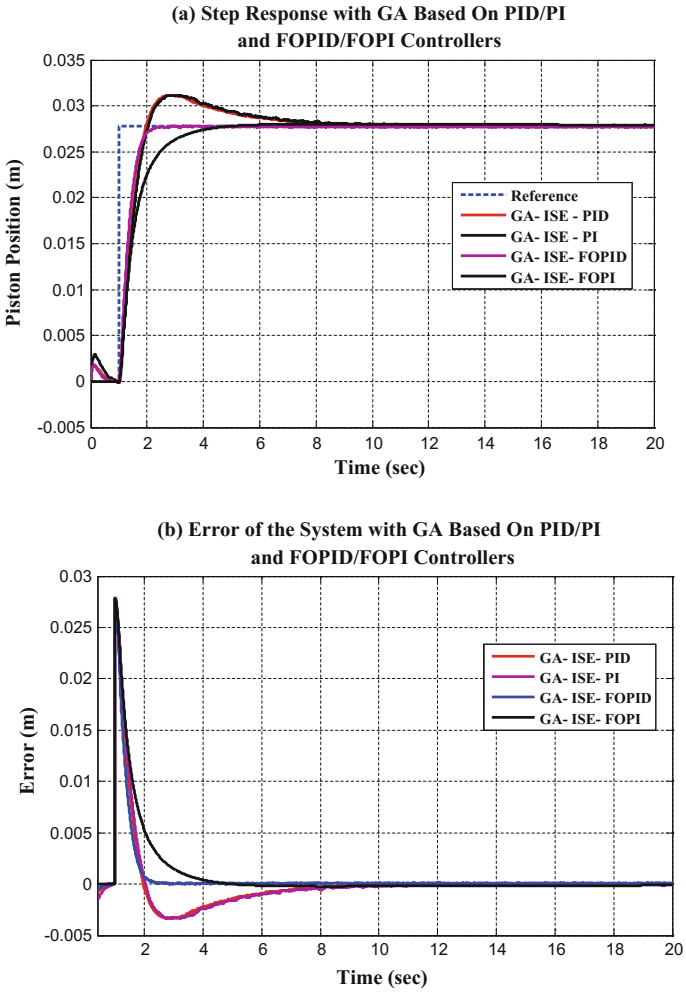

Fig. 29 Piston position and error of experimental HSS with FOPID/FOPI and PID/PI based on GA and ISE

classical controller is shown in Fig. 31. Whereas the profile's changing of the HSS model based on GA with nonlinear controller is displayed in Fig. 32. The figures show that the fractional order controller based on GA has better results in the case of profile changing in relation to other techniques and the system behaves stronger ant changing profile ability.

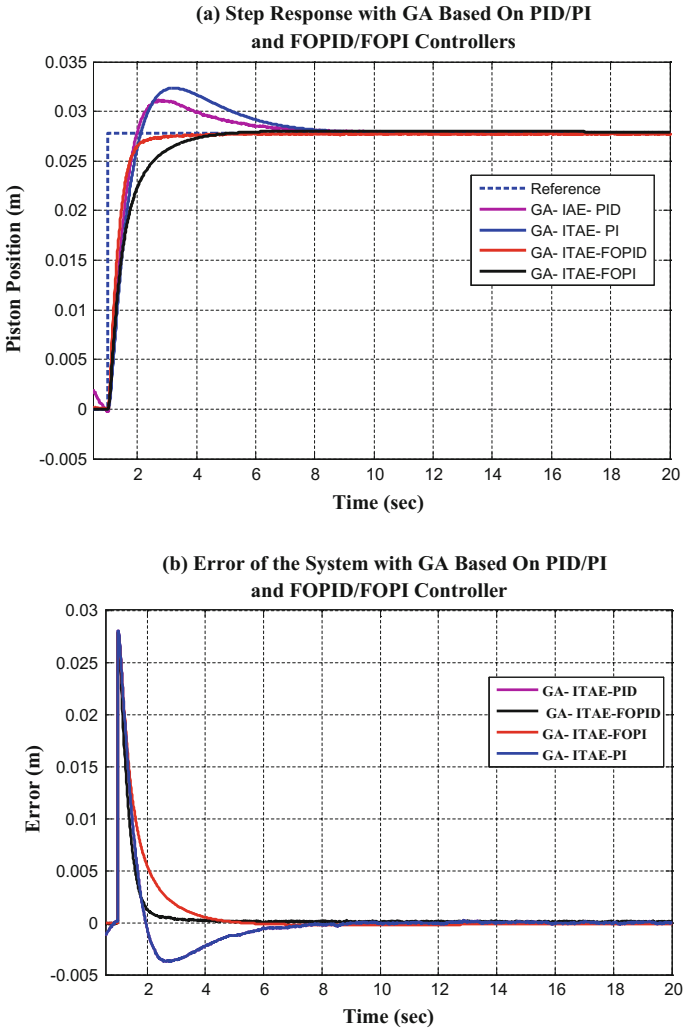

Fig. 30 Piston position and error of experimental HSS with FOPID/FOPI and PID/PI based on GA and ITAE

6.7 Discussion of Experimental Results

The cases of the experimental system depend on the results Table for PSO, AWPSO, GA that illustrated in Table 3. The settling time of the system response based on fractional order controller using GA is the minimum value which around 2.5 s in relation to the other controller results. Moreover there isn't a system overshoot in case of fractional controller in compared with the available overshoot values in conventional controllers. In addition, the settling time of the system

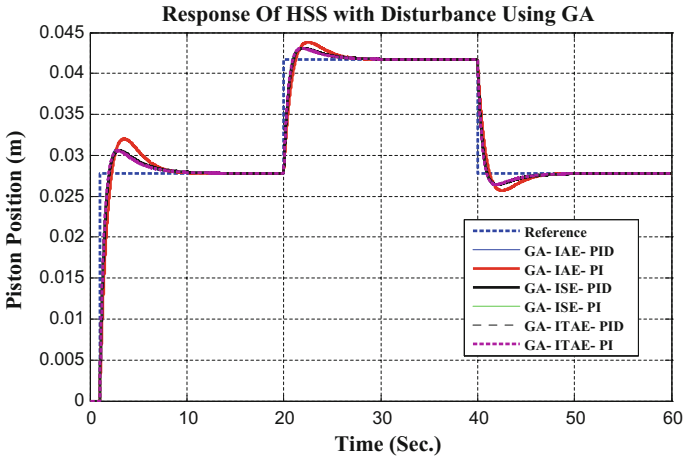

Fig. 31 Response of HSS simulation model with 50% changing in profile based on GA

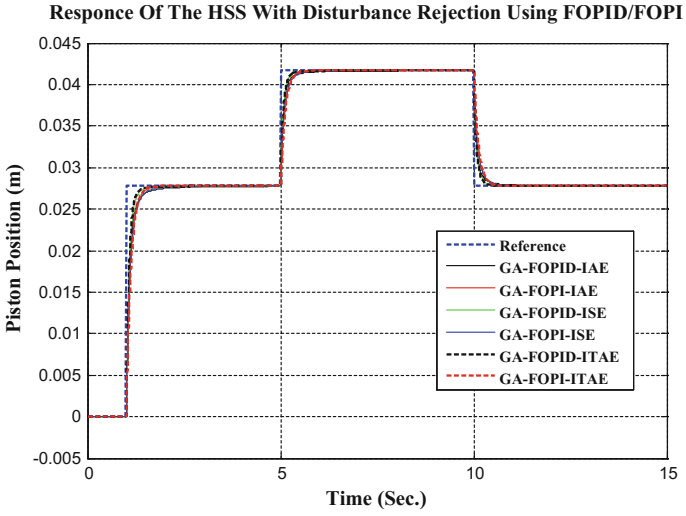

Fig. 32 Response of HSS simulation model with 50% changing in profile based on GA and fractional order controller

response anchored in fractional order controller is the minimum value which approximately 2.5 s with regard to the other results. Additionally, there isn't a system overshoot in case of fractional order controller compared with available system overshoot in the conventional controllers. The settling time of the system response based on fractional order controller is the minimum value which around 2.5 s corresponding to the other results. Moreover, there isn't a system overshoot in

case of fractional order controller compared with available system overshoot in the other controllers.

The experimental results illustrate that, there isn't systems undershoot for the three performance indices (IAE, ISE and ITAE) in the case of using PID/PI and FOPID/FOPI controllers. When using the same mentioned parameters of the PID/PI and FOPID/FOPI controllers in Table 3, the Fractional Order controller that based on GA technique give an efficient sinusoidal wave tracking, where it gives an acceptable cross correlation coefficients. On a global analysis to the responses, it is found that the nonlinear controller or the fractional order controller based on GA is the better controller than classical controller in determination the best parameters of the projected controller. On the way, the settling time and system overshoot of the three performance indices in case of Fractional Order PID (FOPID) controller is the minimum value compared with the other results. In fact the fractional controller provides its robustness in reducing the settling time and overshoot from available overshoot value to non overshoot. It is also found that there isn't system undershoot for all the optimization techniques. In addition, the used FOPID gives a better system response and results compared with FOPI controller results.

6.8 *Effects of Changing Reference Profile for the Experimental HSS*

The same changing in profile signal that has been added in the previous signal is also has been added in experimental system. The changing in profile reference based on GA with classical controller is shown in Fig. 33. Whereas the changing in

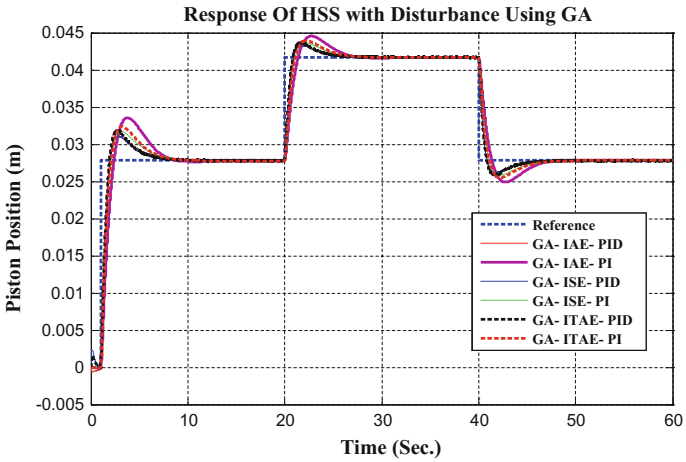

Fig. 33 Response of experimental HSS with 50% changing in profile based on GA

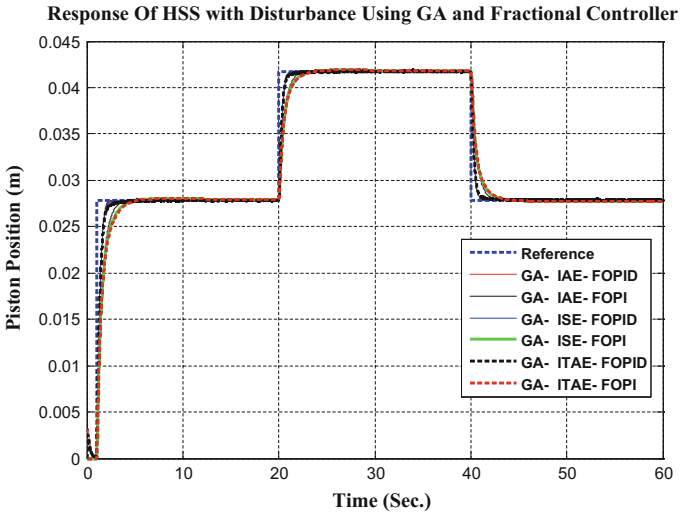

Fig. 34 Response of experimental HSS with 50% changing in profile based on GA and fractional order controller

profile of the HSS model based on GA with nonlinear controller is displayed in Fig. 34. The figures illustrate that the fractional order controller based on GA has better resistance the changing in profile with regard to conventional controllers. It also shows that the system behaves stronger ant changing in profile ability.

6.9 Sensitivity of HSS Parameters

The hydraulic systems have many numbers of perturbations in parameters such as perturbation in supply pressure, Coulomb friction and viscous friction. It was assumed that the system parameters have a perturbation of 20%. Tables 4 and 5 show the settling time and system overshoots of the position control of HSS according to the perturbation of the supply pressure, viscous and coulomb frictions. The simulation and experimental results show that the settling time and system overshoots are still around the same values in case of nominal parameters. It also shows that the proposed controller based on the GA technique have the desired robustness to system uncertainties such as the perturbation of the viscous friction, Coulomb friction and pump's supply pressure. In addition it shows that the fractional order controller is still give good time performance with compared to classical controllers.

Table 4 Time performance of HSS due to supply pressure sensitivity

Tuning Method	Performance Index	Controller Type	Simulation Model of HSS				Experimental HSS			
			Increasing in Supply Pressure by 20 %		Decreasing in Supply Pressure by 20 %		Increasing in Supply Pressure by 20 %		Decreasing in Supply Pressure by 20 %	
			Settling time (sec.)	Over Shoot (%)	Settling time (sec.)	Over Shoot (%)	Settling time (sec.)	Over Shoot (%)	Settling time (sec.)	Over Shoot (%)
GA	IAE	PID	6.192	11.21	6.99	12.81	6.62	11.01	6.93	11.91
		FOPID	1.553	1.1	1.95	1.98	2.02	No O.S	2.52	No O.S
		PI	7.12	17.9	7.80	19.87	7.13	18.1	7.8516	19.7
		FOPI	2.23	No O.S	2.873	No O.S	3.17	1	3.17	1
	ISE	PID	6.446	10.2	6.864	12.85	6.96	10.89	7.6548	12.97
		FOPID	1.445	1.34	1.984	1.94	2.07	No O.S	2.578	No O.S
		PI	6.724	10.97	7.45	12.47	8.05	10.89	8.659	12.87
		FOPI	2.482	1.24	3.28	1.84	3.71	0.5	3.95	1.75
	ITAE	PID	5.88	13.53	6.88	15.63	6.24	13.12	6.98	15.39
		FOPID	1.60	0.61	2.10	1.61	2.54	No O.S	2.98	No O.S
		PI	6.62	13.16	7.92	14.96	7.336	16.18	7.336	16.18
		FOPI	2.595	No O.S	3.69	No O.S	3.87	0.62	4.56	1.71

Table 5 Time performance of HSS due to friction parameters sensitivity

Tuning Method	Performance Index	Controller Type	Simulation Model of HSS				Simulation Model of HSS			
			Increasing in Viscosity Friction by 20 %		Decreasing in Viscosity Friction by 20 %		Increasing in Coulomb Friction by 20 %		Decreasing in Coulomb Friction by 20 %	
			Settling time (sec.)	Over Shoot (%)	Settling time (sec.)	Over Shoot (%)	Settling time (sec.)	Over Shoot (%)	Settling time (sec.)	Over Shoot (%)
GA	IAE	PID	6.611	10.43	6.611	10.43	6.614	10.432	6.613	10.432
		FOPID	1.775	1.6	1.769	1.69	1.776	1.68	1.775	1.6
		PI	6.952	15.64	6.955	15.66	6.953	15.63	6.952	15.64
		FOPI	2.735	No O.S	2.736	No O.S	2.736	No O.S	2.736	No O.S
	ISE	PID	6.95	11.96	6.955	11.97	6.955	11.97	6.955	11.97
		FOPID	1.775	1.5	1.775	1.5	1.775	1.5	1.775	1.5
		PI	6.916	11.96	6.95	11.96	6.946	11.96	6.916	11.96
		FOPI	2.665	No O.S	2.665	No O.S	2.665	No O.S	2.665	No O.S
	ITAE	PID	5.984	15.04	5.984	15.04	5.984	15.04	5.984	15.04
		FOPID	1.915	1	1.918	1	1.916	1	1.918	1
		PI	6.843	7.58	6.845	7.59	6.844	7.582	6.846	7.584
		FOPI	2.987	No O.S	2.988	No O.S	2.979	No O.S	2.9799	No O.S

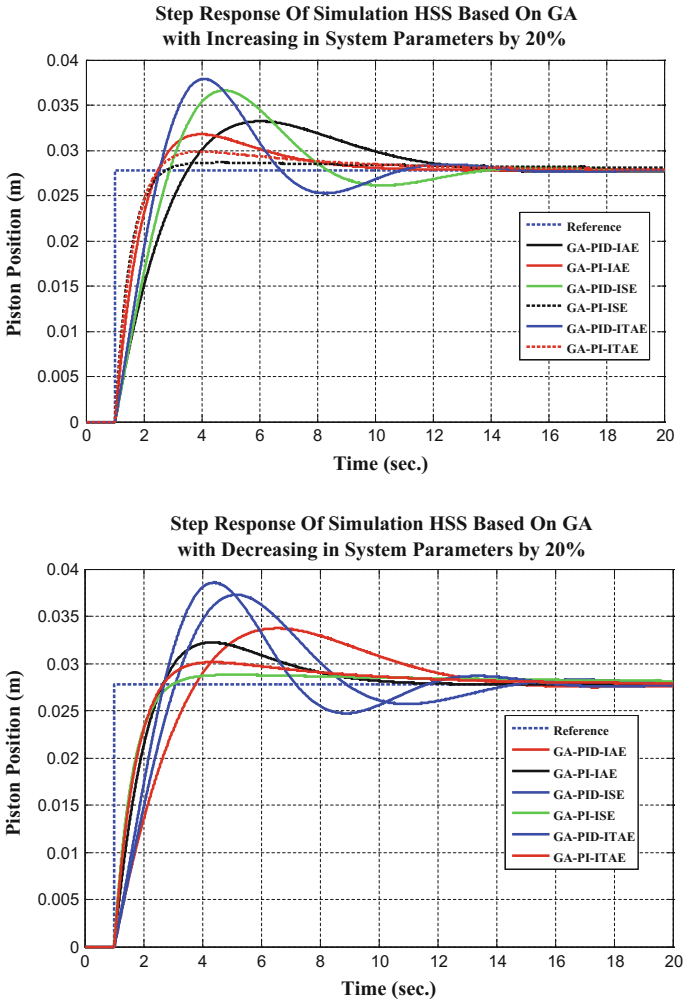

Fig. 35 Step response of simulation HSS based on GA with increasing and decreasing in system parameters

After a deep study of position control of HSS, The recommended controller that gives good time performance, tracking the change in reference profile and robust controller for parameters sensitivity is the fractional order controllers. Figures 35 and 37 present the system response based on GA in case of increasing and decreasing in HSS parameters for conventional controllers. While Figs. 36 and 38 illustrate the system response based on GA and fractional order controllers in case of parameters sensitivity in HSS for the simulation HSS model and experimental hardware respectively.

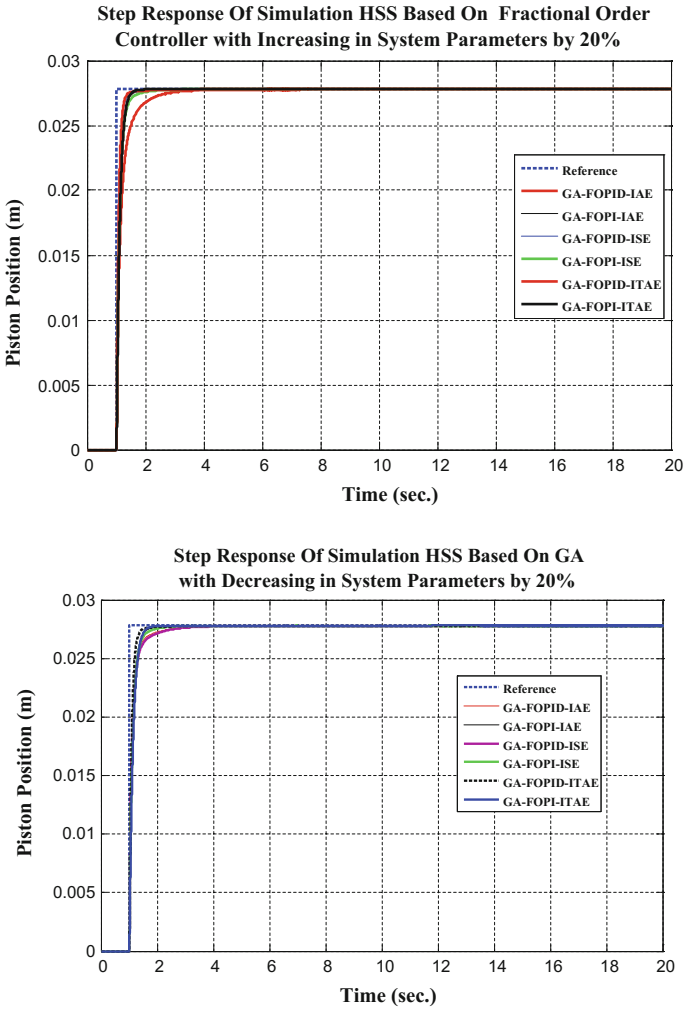

Fig. 36 Step response of simulation HSS based on FOPID/FOPI with increasing and decreasing in system parameters

6.10 Validation Between Simulation and Experimental Results

The main objective of this Section is to illustrate the convergence and validation of results and graphics between the methods, which represents the Hydraulic Servo System (HSS). The results show that a good validation between the following method.

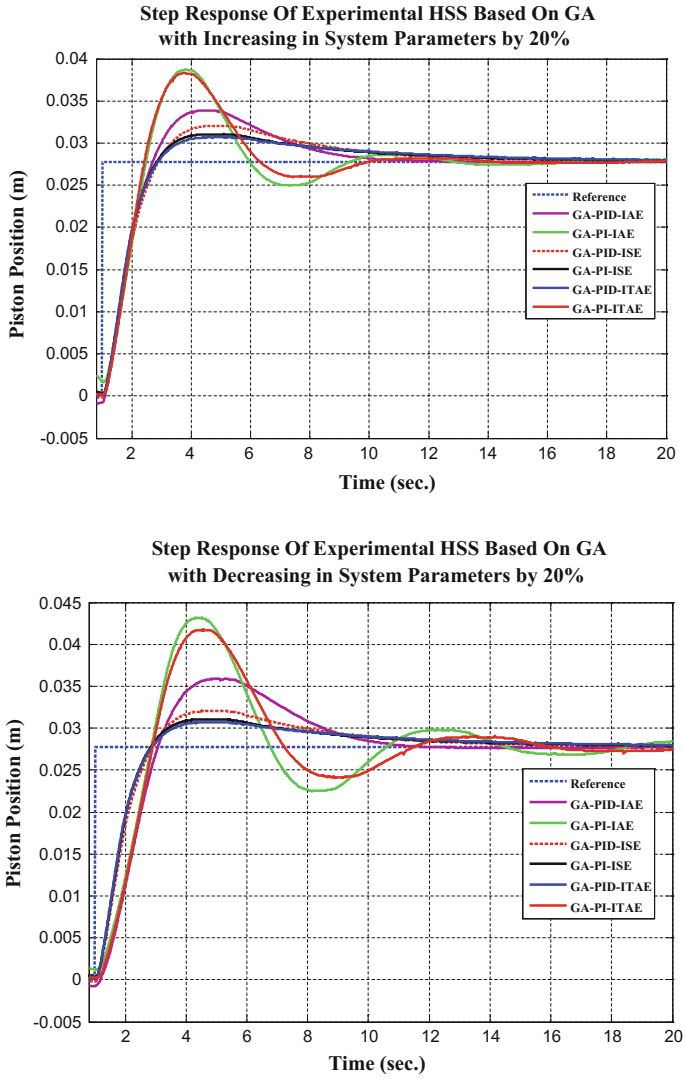

Fig. 37 Step response of experimental HSS based on GA with increasing and decreasing in system parameters

I. Simulation model based on physical laws.
II. Experimental system.
III. Identified model based on input–output data.

The decision of good validation between the above mentioned models is based on that there are a small deviation between the settling time, overshoot and graphs. Figures 39 and 40 show the validation of the results using PID/FOPID controllers based on GA.

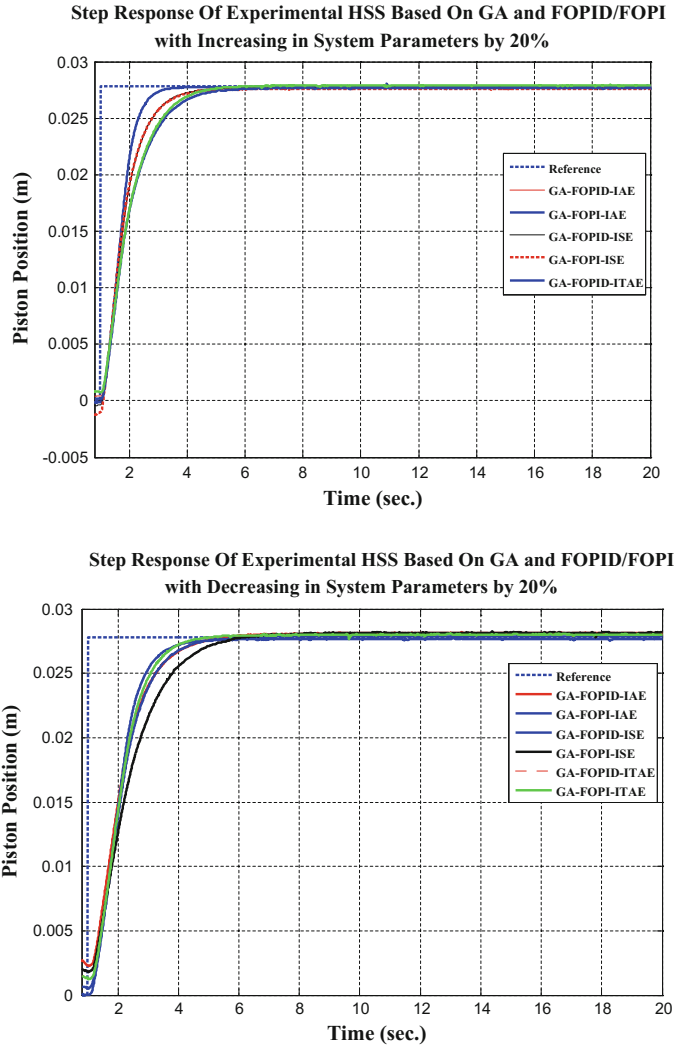

Fig. 38 Step response of experimental HSS based on FOPID/FOPI with increasing and decreasing in system parameters

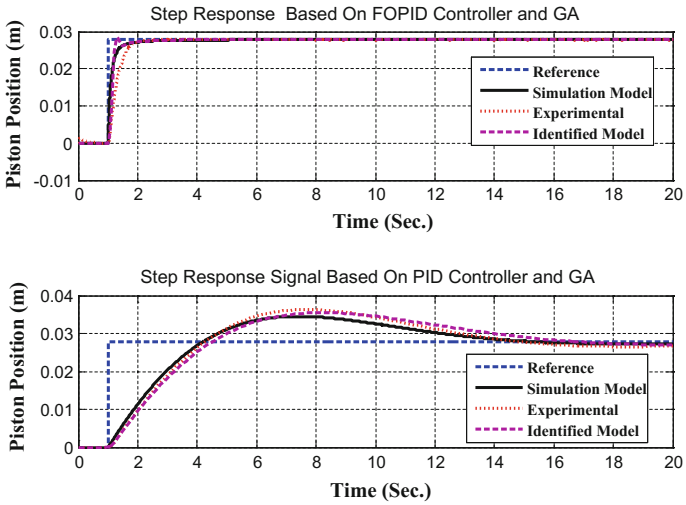

Fig. 39 Validation of step response results using GA

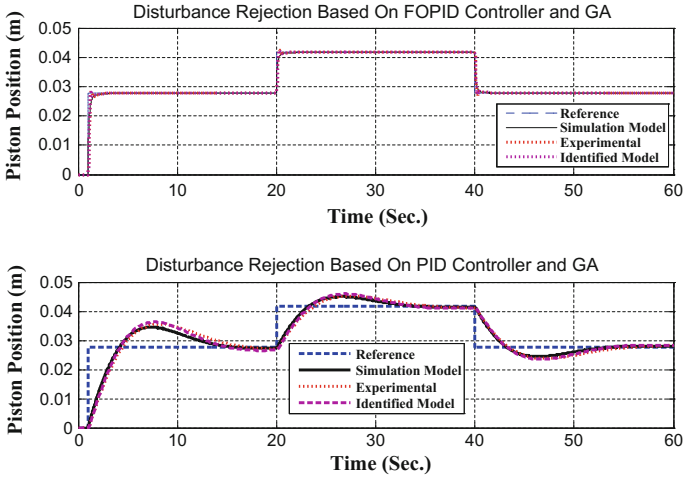

Fig. 40 Validation of disturbance results using GA

7 Conclusion

This chapter presents application of GA to design the following controllers;

(a) PID/PI controllers.
(b) Fractional Order PID/PI controllers.

This design is implemented on simulation model and real time of Position Control for Hydraulic Servo System. The utilized optimization technique and tuning method in this research is Genetic Algorithm (GA).

A SIMULINK model for a typical electro-hydraulic servo system was implemented and modified which included major nonlinearities and was verified on an experimental system. The hardware components are related to Bosch REXROTH German Company. The HSS plays an important role in the industrial applications such as the machine tool industry, material handling, mobile equipment, plastics, steel plants, oil exploration and automotive testing, so it is important to design a robust control system in this field. The experimental and simulation model of HSS are considered as a single optimization problems. The three performance indices (IAE, ISE and ITAE) have been used as the objective functions in GA. Defining the objective function for the system depends on the dynamics of the system and the desired performance for the system. The results demonstrated that the minimum settling time in case of GA based on conventional and fractional order controllers are 5.98 s and 1.64 s respectively. In addition, in case of GA based on classical and fractional controller, the minimum settling times are 6.404 and 2.017 s respectively. A changing in profile signal with 50% from the set point signal are is applied to HSS model and real time system with GA, it showed that there are a spikes and dips in GA based on conventional controller. But in case of fractional order controller, it showed that better achievement of changing in profile in relation to other techniques and the system behaves stronger ant changing in profile ability.

The simulation and experimental results showed that the nonlinear controller or fractional order controller achieved a desired performance for position control of HSS by reducing settling time and overshoots with measurable values. There are no spikes or dips appeared in the output response, while the system reached steady state smoothly compared to the other utilized techniques. It also displayed that the system responses of simulation model and experimental system with the fractional order controller based on GA are reliable and robust system with disturbance rejection. Due to the nonlinearities of HSS because of the frictions forces, valve dynamics, oil compressibility and load influence, it is recommended to utilize a non linear controller such Fractional Order Controller to avoid these effects of HSS nonlinearities.

8 Future Work

The simulation and experimental results showed that the fractional order controller achieved better dynamic response of the HSS system accurately tracks the trajectory and remains robust to disturbances. More desirable performance and future work of the HSS system can be achieved by utilizing the following considerations:

- Using conventional controller with Fuzzy Logic Controller (FLC) based on PSO, AWPSO and GA.
- Utilizing fractional order controllers with nonlinear controllers like Fuzzy Logic Controller (FLC) to adequate with the nonlinearities of HSS.
- Implementing a two degree of freedom controller.
- Implementing HSS model for tracking the higher frequency signals.
- Implementing force and pressure trajectory for HSS to be familiar with the operation of HSS.
- Controller design to assurance stability and performance for change from position tracking to pressure/force tracking.
- Design a fractional controller based on GA to achieve better and more desirable performance of the system in terms of pressure and force tracking.
- Design a controller based on PSO, AWPSO and GA with multi objective functions of settling time and overshoots.

References

1. Astrom, K. J., & Hägglund, T. (1995). *PID controllers: Theory, design and tuning* (2nd ed.). Research Triangle Park: International Society of Automation. ISBN 1-55617-516-7.
2. Ahmed, O. A. (2009). Control of fluid power system-nonlinear fuzzy control for force tracking of electro-hydraulic servo system. Master Thesis, Faculty of Engineering (at Shoubra), Benha University, Egypt.
3. Aly, A. A. (2011). PID parameters optimization using genetic algorithm technique for electro hydraulic servo control system. *Intelligent Control and Automation*, *2*(02), 69–76.
4. Azar, A. T., & Serrano, F. E. (2014). Robust IMC-PID tuning for cascade control systems with gain and phase margin specifications. *Neural Computing and Applications*, *25*(5), 983–995. doi:10.1007/s00521-014-1560-x.
5. Azar, A. T., & Serrano, F. E. (2015). Design and modeling of anti wind up PID controllers. In Q. Zhu & A. T Azar (Eds.), *Complex system modelling and control through intelligent soft computations*. Studies in Fuzziness and Soft Computing (Vol. 319, pp. 1–44). Germany: Springer. doi:10.1007/978-3-319-12883-2_1.
6. Azar, A. T., & Vaidyanathan, S. (2015). *Chaos modeling and control systems design*. Studies in Computational Intelligence (Vol. 581). Germany: Springer. ISBN 978-3-319-13131-3.
7. Bonchis, A., Corke, P. I., Rye, D. C., & Ha, Q. P. (2001). Variable structure methods in hydraulic servo systems control. *Automatica*, *37*(4), 589–595.
8. Chen, H. M., Shen, C. S., & Lee, T. E. (2013). Implementation of precision force control for an electro-hydraulic servo press system. In *Proceeding of Third International Conference on Intelligent System Design and Engineering Applications (ISDEA)* (pp. 854–857). IEEE.

9. Das, S. (2008). *Functional fractional calculus for system identification and controls*. Berlin, Heidelberg: Springer.
10. Edvard, D., & Uroš, Ž. (2011). An intelligent electro-hydraulic servo drive positioning. *Strojniškivestnik-Journal of Mechanical Engineering*, *57*(5), 394–404.
11. Elbayomy, K. M., Zongxia, J., & Huaqing, Z. (2008). PID controller optimization by GA and its performances on the electro-hydraulic servo control system. *Chinese Journal of Aeronautics*, *21*(4), 378–384.
12. Essa, M., Aboelela M. A. S., & Hassan, M. A. M. (2014a). Position control of hydraulic servo system using proportional-integral-derivative controller tuned by some evolutionary techniques. *Journal of Vibration and Control*, 1077546314551445.
13. Essa, M., Aboelela M. A. S., & Hassan, M. A. M. (2014b). Position control of hydraulic servo systems using evolutionary techniques. Master thesis, Faculty of Engineering (Cairo University), Egypt.
14. Goldberg, D. E., & Holland, J. H. (1988). Genetic algorithms and machine learning. *Machine learning*, *3*(2), 95–99. doi:10.1023/A:1022602019183.
15. Jelali, M., & Kroll, A. (2012). *Hydraulic servo-systems: Modeling, identification and control*. Springer, London Ltd. ISBN 978-1-4471-1123-8.
16. Kao, C. C. (2009). Applications of particle swarm optimization in mechanical design. *Journal of Gaoyuan University*, *15*, 93–116.
17. Kim, J.-S., Kim, J.-H., Park, J-M., Park, S.-M., Choe, W.-Y., & Heo, H. (2008). Auto tuning PID controller based on improved genetic algorithm for reverse osmosis plant. *World Academy of Science, Engineering and Technology*, *47*(2), 384–389.
18. Ljung, L. (2010). System Identification Toolbox 7 Getting started guide. http://www.mathworks.com.
19. Maneetham, D., & Afzulpurkar, N. (2010). Modeling, simulation and control of high speed nonlinear hydraulic servo system. *Journal of Automation Mobile Robotics and Intelligent Systems, 4*, 94–103.
20. Mahdi, S. M. (2012). Controlling a nonlinear servo hydraulic system using PID controller with a genetic algorithm tool. *IJCCCE, 12*(1), 42–52.
21. Mathwork. (2014). Simulink Design Optimization Toolbox. http://www.mathworks.com.
22. Mannesmann Rexroth. (2005) 4/3-way high response directional valve direct actuated, with electrical position feedback Type 4WRSE. http://www.boschrexroth.com.
23. Mahony, T. O., Downing, C. J., & Fatla, K. (2000). Genetic algorithm for PID parameter optimization: Minimizing error criteria. *Process Control and Instrumentation*, 148–153.
24. Machado, J. T. (1997). Analysis and design of fractional-order digital control systems. *Systems Analysis Modeling Simulation*, *27*(2–3), 107–122.
25. Md Rozali, S., Rahmat, M. F. A., Husain, A. R., & Kamarudin, M. N. (2014). Design of adaptive back stepping with gravitational search algorithm for nonlinear system. *Journal of Theoretical and Applied Information Technology (JATIT)*, *59*(2), 460–468.
26. Merritt, H. E. (1967). *Hydraulic control systems*. New York: Wiley. ISBN 0-471-59617-5.
27. Mihajlov, M., Nikolić, V., & Antić, D. (2002). Position control of an electro-hydraulic servo system using sliding mode control enhanced by fuzzy PI controller. *Facta Universitatis-Series: Mechanical Engineering*, *1*(9), 1217–1230.
28. National Instrument. (2002). DAQ NI 6013/6014 User Manual. http://www.ni.com.
29. Nelles, O. (2013). *Nonlinear system identification: From classical approaches to neural networks and fuzzy models*. Berlin, Heidelberg: Springer. ISBN 978-3-642-08674-8.
30. Olranthichachat, P., & Kaitwanidvilai, S. (2011). Design of optimal robust PI controller for electro-hydraulic servo system. *Engineering Letters, 19*(3), 197–203.
31. Olranthichachat, P., & Kaitwanidvilai, S. (2011b). Structure specified robust H∞ loop shaping control of a MIMO electro-hydraulic servo system using particle swarm optimization. In *Proceedings of the International Multi Conference of Engineers and Computer Scientists* (Vol. 2).
32. Podlubny, I. (1999). Fractional-order systems and $PI^{\lambda}D^{\delta}$ controllers. *IEEE Transactions on Automatic Control, 44*(1), 208–214.

33. Puangdownreong, D., & Sukulin, A. (2012). Obtaining an optimum PID controllers for unstable systems using current search. *International Journal of Systems Engineering, Applications & Development 6*(2), 188–195.
34. Rydberg, K. E. (2008). Hydraulic servo systems. TMHP51 fluid and mechanical engineering systems. *Linköping University*, 1–45.
35. Roozbahani, H., Wu, H., & Handroos, H. (2011). Real-time simulation based robust adaptive control of hydraulic servo system. In *Proceeding of IEEE International Conference on Mechatronics (ICM)*, 779–784.
36. Saad, M. S., Jamaluddin, H., & Darus, I. Z. (2012). PID controller tuning using evolutionary algorithms. *WSEAS Transactions on Systems and Control*, *7*(4), 139–149.
37. Sirouspour, M. R., & Salcudean, S. E. (2000). On the nonlinear control of hydraulic servo-systems. In *IEEE International Conference on Robotics and Automation Proceedings. ICRA'00* (Vol. 2, pp. 1276–1282). IEEE.
38. Sivanandam, S. N., & Deepa, S. N. (2007). *Introduction to genetic algorithms*. Berlin, Heideberg, New York: Springer. ISBN 978-3-540-73189-4.
39. Sohl, G. A., & Bobrow J. E. (1999). Experiments and simulations on the nonlinear control of a hydraulic servo system. *IEEE Transactions on Control Systems Technology*, *7*(2), 238–247.
40. Tooby, J., & Cosmides, L. (1989). Adaption versus phylogeny: The role of animal psychology in the study of human behavior. *International Journal of Comparative Psychology*, *2*(3), 175–188.
41. Tian, J. (2013). Study on control strategy of electro-hydraulic servo loading system. *Indonesian Journal of Electrical Engineering*, *11*(9), 5044–5047.
42. Truong, D. Q., Kwan, A. K., Hung, H. T., & Yoon II, J. (2008). A study on hydraulic load simulator using self tuning grey predictor-fuzzy PID. In *Proceedings of the 17th World Congress the International Federation of Automatic Control (IFAC)* (Vol. 41, No. 2, pp. 13791–13796).
43. Xue, D., Atherton, D. P., & Chen, Y. (2007). *Linear feedback control: Analysis and design with MATLAB* (Vol. 14). Siam.
44. Yao, J. J., Di, D., Jiang, G., & Liu, S. (2012). High precision position control of electro-hydraulic servo system based on feed-forward compensation. *Research Journal of Applied Sciences, Engineering and Technology., 4*(4), 289–298.
45. Yu, M., & Lichen, G. (2013). Fuzzy immune PID control of hydraulic system based on PSO algorithm. *Indonesian Journal of Electrical Engineering*, *11*(2), 890–895.